

NATIONAL RADIO ASTRONOMY OBSERVATORY
CHARLOTTESVILLE, VIRGINIA

ELECTRONICS DIVISION INTERNAL REPORT No.

A METHOD FOR MEASURING AN EQUIVALENT
CIRCUIT OF WAVEGUIDE— MOUNTED DIODES

M. POSPIESZALSKI
AND
S. WEINREB

OCTOBER 1979

NUMBER OF COPIES: 150

A METHOD FOR MEASURING AN EQUIVALENT
CIRCUIT OF WAVEGUIDE - MOUNTED DIODES

TABLE OF CONTENTS		<u>Page</u>
I.	Introduction	1
II.	Diode Mount as a Three Port Junction	3
III.	Schottkey Barrier Diode as a Variable Load and Square Law Detector	7
IV.	Determination of Mount and Diode Equivalent Circuits	9
V.	Example of 2 mm Mixer Analysis	15
	A. Evaluation of a Diode Embedding Circuit.	15
	B. Embedding Network and Mixer Performance.	24
VI.	Errors	24
	A. Measurement Errors	26
	B. Validity of Assumptions.	26
	C. Computation Convergence Error.	27
	D. Error Multiplication Effecting [y] Parameters and Element Values.	27
	E. Error Multiplication Effecting Element Values Only	29
	References	30

APPENDICES

Appendix 1	Summary of Experimental Data on 2 mm Mixers.	31
	A.1.1 D.C. and Low-Frequency Measurements	31
	A.1.2 The Backshort Measurements.	31
	A.1.3 Mixer Measurements.	32
Appendix 2	Computer Programs for Diagnosis of Microwave Mixer Mounts.	40
	A.2.1 Programs for Determining the Mixer Mount Equivalent Circuit.	40
	A.2.2 Programs for Analyzing Mixer Mount Equivalent Circuits.	58

FIGURES

		<u>Page</u>
Figure 1	Example of DC current variation as a function of backshort position for a 110.5 GHz mixer and five different values of bias current	4
Figure 2	Schematic cross-section of a typical millimeter-wave mixer mount.	5
Figure 3(a)	General representation of a lossless three port	6
3(b)	Equivalent circuit of a symmetric mixer mount	6
Figure 4	Equivalent circuits of a diode mount with generator and backshort connected.	6
Figure 5	The measurement setup	10
Figure 6	Electron microscope photographs of the 2 mm mixer mounts.	16
Figure 7	The geometry of the Schottky barrier diodes.	18
Figure 8	The dependence of the diode capacitance C_d on the diode bias voltage V_o	18
Figure 9	The dependence of $\frac{1}{C_d^2}$ on the diode bias voltage V_o	22
Figure 10	The curves of $\frac{\Delta I}{\Delta I_{\max}} = f(Y_{BS} \times Z_G)$ for mixer A computed using values of circuit elements from Table I.	23
Figure 11	The total loss ΔL and loss due to the reflection ΔL_R caused by the embedding circuits of mixers A and B versus resistance R_{RF} presented to the circuit by the pumped diode	25
Figure 12	Measured diode capacitance for a 2 mm mixer mount as a function of bias voltage	28
Figure A.1.	D.C. characteristics of the 2P11 and 2P8-600 diodes	34
Figure A.2.	Dependence of the diode differential resistance on the inverse of the bias current.	35
Figure A.3.	The conversion loss and noise temperature measurement setup used at 152.8 GHz (a) and 201.3 GHz (b).	38

TABLES

Table 1	The measured parameters of the diode and its embedding circuits	20
Table II	The SSB performance of mixers	25
Table III	Element values for 2 mm mixer mount	28
Table A.1.	Summary of backshort measurements on mixer A at 152.8 and 200.3 GHz.	36
Table A.2.	Summary of backshort measurements on mixer B at 152.8 and 200.3 GHz.	37
Table A.3.	The dependence of the signal level needed to produce $\frac{\Delta I_{\max}}{I_B} = 0.1$ at 152.8 GHz	39
Table A.4.	Summary of 4.75 GHz IF_1 SSB mixer performance with pump at 152.8 and 200.3 GHz	39

A Method for Measuring an Equivalent Circuit of Waveguide - Mounted Diodes

M. Pospieszalski* and S. Weinreb**

Abstract - A method of measurement of the embedding circuit and diode parasitics of a semiconductor diode mounted in a waveguide is described. The method is unique in that no instrumentation is required other than an RF signal source, wide-range DC milliammeter, VSWR meter, and a sliding short (usually built into the mount) with a linear position scale. Thus the method is applicable at millimeter wavelengths and can be performed upon a mixer which is mounted in a system or is at cryogenic temperatures. The basic technique is to apply a small microwave signal to the mount and measure the diode current as a function of sliding short position for several different values of d-c bias voltage. The method is demonstrated by analysis of two 140-220 GHz mixer mounts.

I. INTRODUCTION

A common problem in present day microwave engineering is the characterization of the coupling network and parasitics of a diode mounted in waveguide. Tools for attacking this problem are

* National Radio Astronomy Observatory, Charlottesville, Va, on leave of absence from Warsaw Technical University, Institute of Electronic Fundamentals, Warsaw, Poland.

** National Radio Astronomy Observatory, operated by Associated Universities Inc., under contract to National Science Foundation.

theoretical analyses of the waveguide-to-gap coupling network given by Eisenhart and Kahn [1] and Joshi and Cornic [2], microwave measurement methods of diode parameters, such as described by DeLoach [3], large scale model measurements, such as those applied to millimeter wave mixers by Held and Kerr [4,5], and a recently published reflectometer technique by Hagström and Kollberg [6].

In our work concerning millimeter wave mixer development, all of the above techniques are of some usefulness. However, we desired a diagnostic technique which can be applied to a completed mixer mount, including diode, and give detailed information as to why the mount was particularly good or bad. The technique should answer questions such as "What impedance is presented to diode by the embedding circuit?," "Are the losses due to the diode parasitic elements too large?," "What behavior may be expected at a nearby frequency?"

During tests of various mixers, it was noted that curves of rectified diode current versus backshort position varied in appearance according to the frequency and diode. The analysis of these curves for a diode with sufficient LO power for good mixer performance is a quite complex non-linear problem [4]. However, it was recognized that diode current vs. backshort position curves could be measured for LO currents small compared to DC bias current and analyzed by conventional linear network methods, plus square-law detector theory as outlined in Sections II and III of this paper. Furthermore, by measuring this curve for several values of DC bias current much information about the diode and coupling network could be obtained.

A typical set of these curves made under the small LO condition, and for five different DC bias voltages is shown in Fig. 1. (All measurements made in this paper are at constant DC bias voltage, but are described by the DC current for zero LO power.) It will be shown in Section IV that each curve is proportional to $1/|Y_{IN} + Y_g + Y_{BS}|^2$ where $Y_{IN} + Y_{BS}$ is the input admittance of the waveguide port, Y_g is the generator source admittance, and Y_{BS} is the backshort admittance. The latter two quantities are known, and thus, Y_{IN} is determined by measuring the peak and width of each curve. It will also be shown that a mount equivalent circuit can be determined by measuring Y_{IN} for five different values of differential diode conductance, g_d ; i.e., for five different values of DC bias current.

II. DIODE MOUNT AS A THREE PORT JUNCTION

A cross section of a typical mixer mount is shown in Fig. 2. This mount can be considered as a microwave network having three ports connected to: 1) generator, 2) backshort, and 3) diode. Any lossless, reciprocal three port junction can be represented at a given frequency by the equivalent circuit shown in Fig. 3a [8,9]. This circuit consists of 7 independent elements, although it is obvious that one transformer may be assigned an arbitrary turn ratio. It is most convenient to set $n_3 = 1$. As lengths l_1 and l_2 may be set equal to zero by a proper choice of reference planes in the generator and backshort arms, only 4 elements n_1 , n_2 , Y , Z_s need to be determined. It is also obvious that for reference planes close to the diode, so that the three port excludes the waveguide-height transformer, the mount is symmetrical and

110.5 GHZ CONTACTING BACK-SHORT
MTR X 208-500 6/29/79

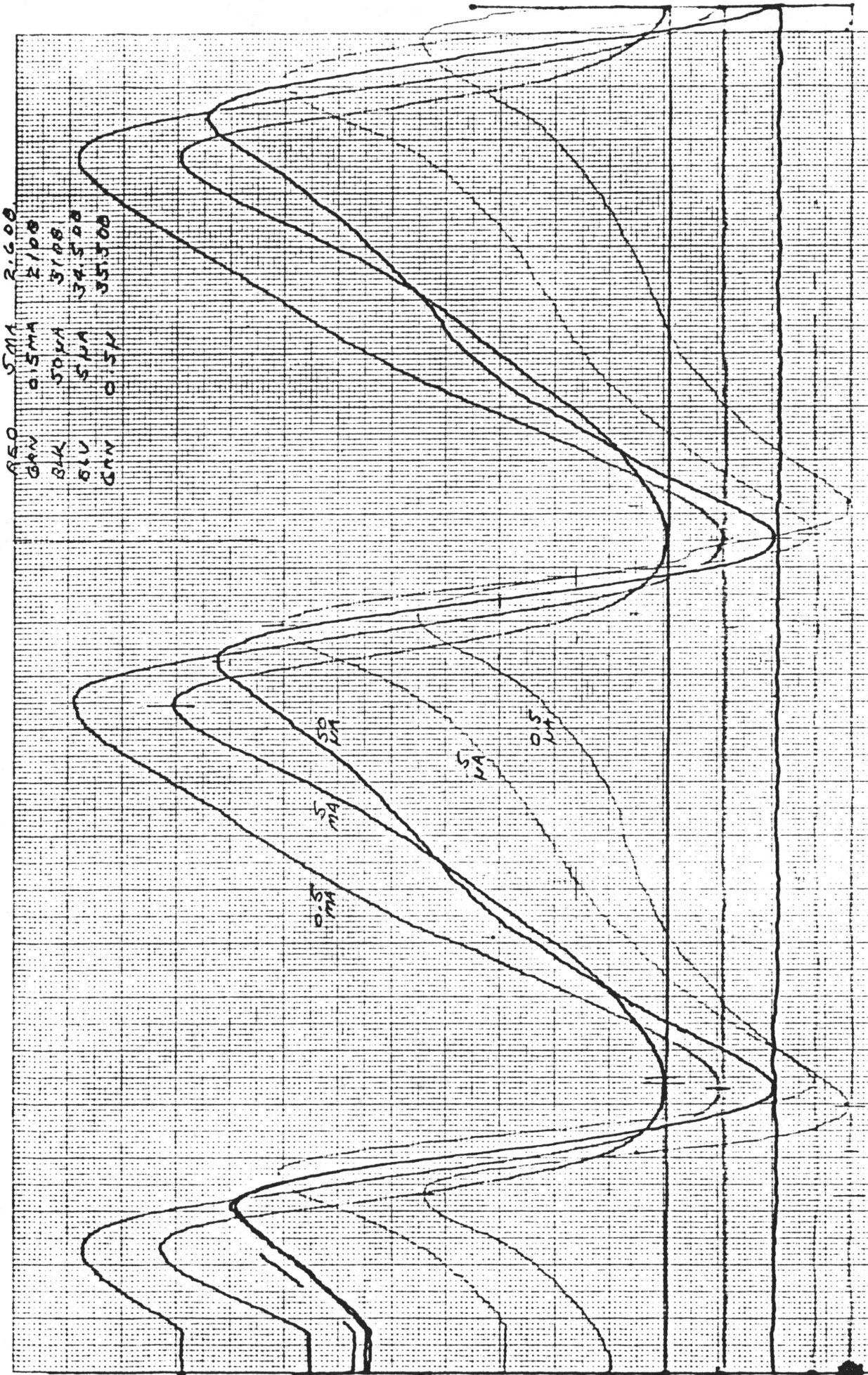


Figure 1 - Example of DC current variation as a function of backshort position for a 110.5 GHz mixer and five different values of bias current. The baselines for each curve represent the bias current with no microwave signal applied and have been offset from each other. The microwave power has been adjusted for each bias current so that the peak change of each curve is ~ 10% of the bias current.

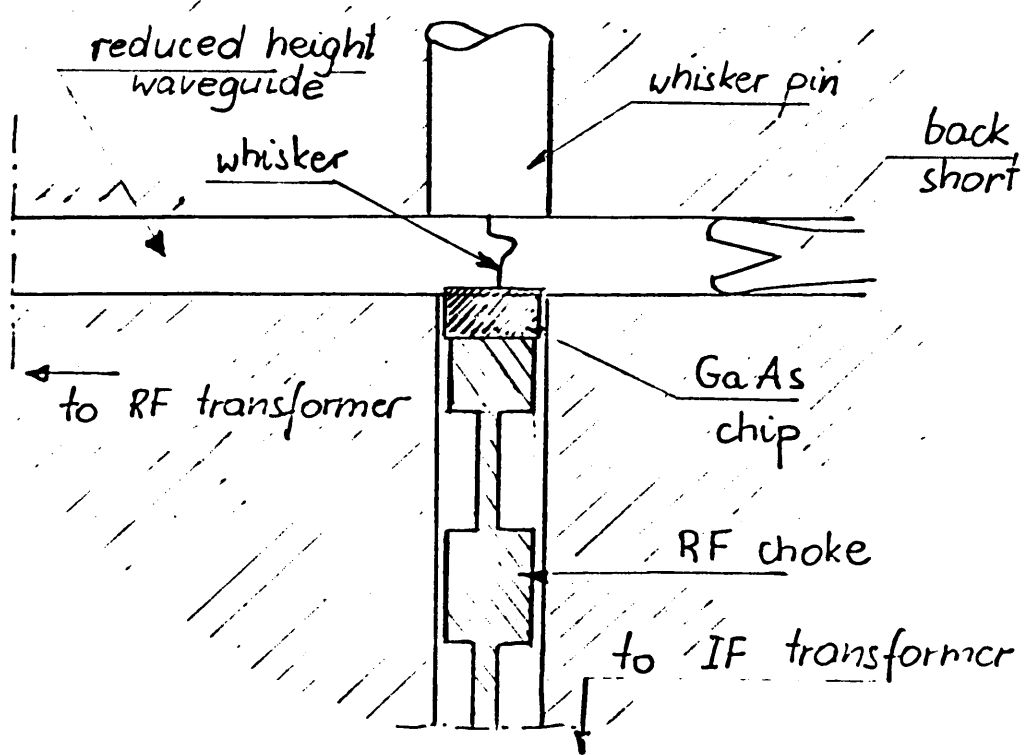


Fig. 2. Schematic cross-section of a typical millimeter-wave mi mount.

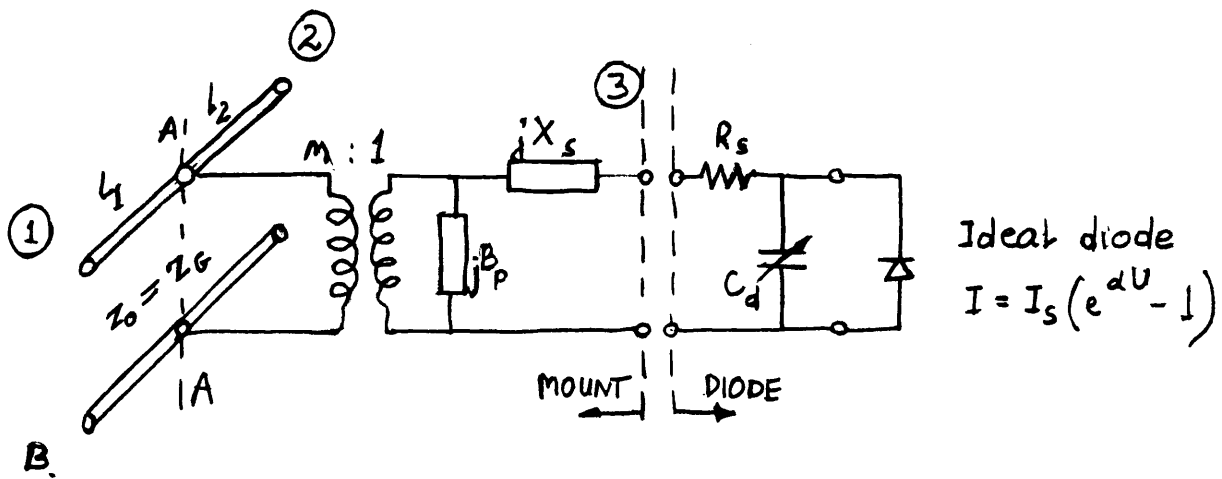
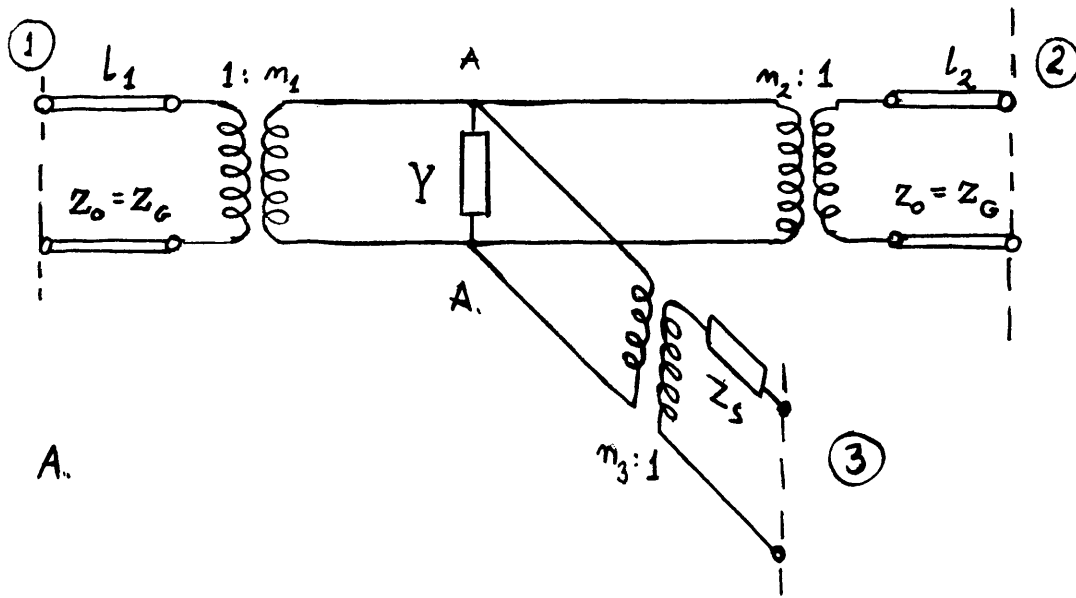


Fig. 3. (a) General representation of a lossless three-port.
 (b) Equivalent circuit of a symmetric mixer mount.

$n_1 = n_2$. This requires the assumption that any deviations from symmetry in the diode mounting structure are small compared to a wavelength.

With this symmetry assumption and some simple transformations, the circuit can be changed to that of Fig. 3(b) which contains 5 independent elements, i.e.: l_1 , l_2 , n , B_p , and X_s .

Again, only three elements-- n , B_p , and X_s need to be determined. It is also clear that the validity of the equivalent circuit is not affected by the choice of the particular definition of the waveguide characteristic impedance Z_G , as it can be changed by a change of the value of n . However, following previous works on waveguide mounts, the power-voltage definition of Schelkunoff is chosen throughout this paper; that is,

$$Z_G = \sqrt{\frac{\mu}{\epsilon}} \cdot \frac{2b}{a} \cdot \frac{\lambda_g}{\lambda} \quad (1)$$

where all the symbols have their conventional meaning.

III. SCHOTTKY BARRIER DIODE AS A VARIABLE LOAD AND SQUARE LAW DETECTOR.

The equivalent circuit of a Schottky barrier diode is also shown in Fig. 3(b). The $i - v$ characteristic of the ideal-diode portion of the model can be very well determined by dc and low frequency measurements, and should be equally valid at millimeter wavelengths. This characteristic is described by:

$$i = I_s (e^{\alpha v} - 1) \quad (2)$$

$$\text{and} \quad \alpha = \frac{q}{\eta k T} \quad (3)$$

where: I_s = diode saturation current
 q = electronic charge
 κ = Boltzmann's constant
 T = absolute temperature
 η = junction ideality factor

For small RF signals [10] the diode biased at a certain operating point (I_B, V_B) can be considered as a linear conductance,

$$g_{do} = \alpha I_B \quad (4)$$

and a square law detector having small signal current responsivity,

$$\beta_o = \frac{\Delta I}{P} = \frac{\alpha}{2} \quad (5)$$

where: P = RF power absorbed by the diode,

ΔI = increase in dc current of the diode due to the presence of RF signal.

The knowledge of the i-v characteristic of the diode allows both the computation of the value of the resistance terminating the network of Fig. 3(b), and also the measurement, through ΔI , of the amount of power absorbed by this load. Equations (4) and (5) are valid for small signals applied to the diode. To evaluate how small the signal must be a given error, we use the following relations [6]:

$$\frac{g_d}{g_{do}} = \frac{2I_1(\alpha V_p)}{\alpha V_p} = 1 + \frac{(\alpha V_p)^2}{2^2 1! 2!} + \frac{(\alpha V_p)^4}{2^4 2! 3!} + \dots \quad (6)$$

$$\frac{\Delta I}{I_B} = I_o(\alpha V_p) - 1 = \frac{(\alpha V_p)^2}{2^2 (1!)^2} + \frac{(\alpha V_p)^4}{2^4 (2!)^2} + \dots \quad (7)$$

where: V_p - the amplitude of a sinusoidal voltage applied to the diode,
 g_d - diode conductance defined as a ratio of the fundamental
frequency current and voltage amplitudes,
 I_0, I_1 - the modified Bessel junction of the first kin.

Under small signal approximations, (6) and (7) can be combined
to give

$$\frac{g_d}{g_{d0}} \approx 1 + \frac{\Delta I}{2I_B} \quad (8)$$

Equation (8) can be used either to correct values of g_0 needed in the
analysis, or to set an upper limit upon $\Delta I | I_B$ to allow using g_{d0} in
place of g_0 .

IV. DETERMINATION OF MOUNT AND DIODE EQUIVALENT CIRCUITS

The diode can be represented as an ideal diode as described above
coupled to a voltage-dependent diode capacitance, C_D , and series resis-
tance R_S as shown in Fig. 3(b). We wish to determine these two quanti-
ties, and the coupling network parameters.

Connecting generator and backshort to the circuit of Fig. 3(b)
results in the equivalent circuit shown in Fig. 4(a). Since no micro-
wave power is coupled to the diode (i.e., $\Delta I = 0$) for positions of the
backshort where $Y_{BS} = \infty$, a reference plane for measurement of backshort
position is established and Y_{BS} is given by:

$$Y_{BS} = -j Y_G \cot \frac{2\pi l}{\lambda g} \quad (9)$$

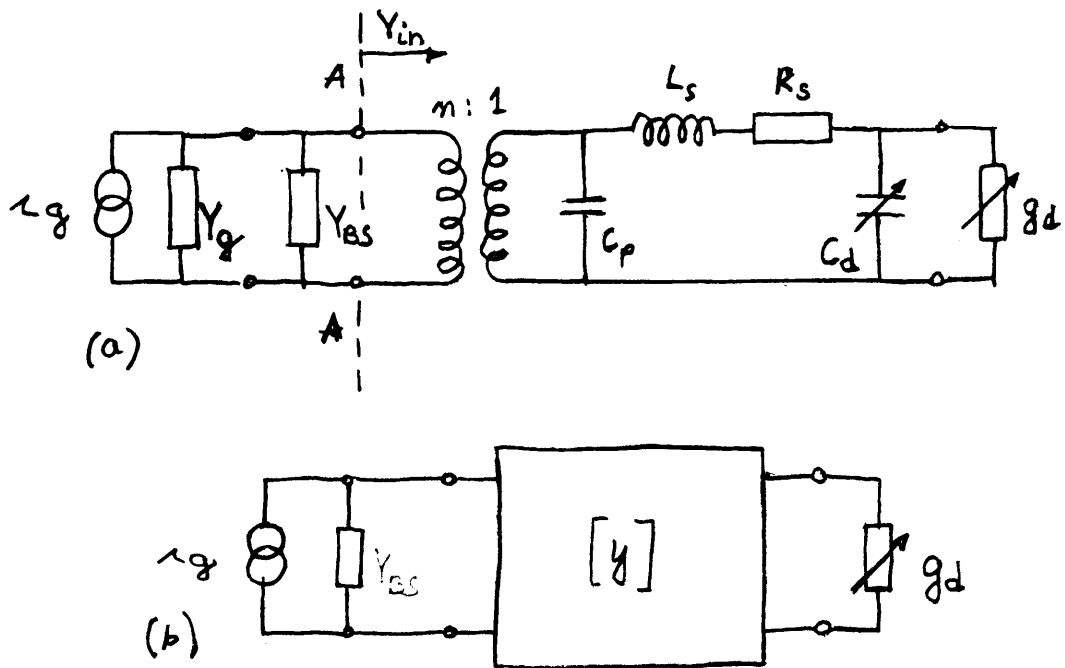


Fig. 4. Equivalent circuits of a diode mount with generator and backshort connected.

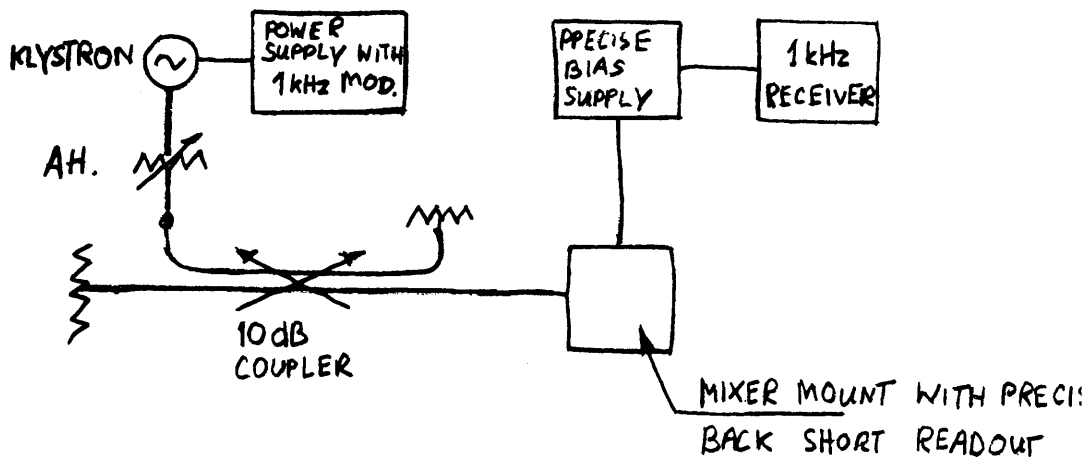


Fig. 5. The measurement setup.

where l is the distance between the backshort position and the next position towards the diode where ΔI is a null, λ_g is the guide wavelength, and $Y_G = Z_G^{-1}$.

If the mount is symmetric and the generator is well matched, $Y_g = Y_G$ and only three parameters of coupling network: n , B_p , and X_s , need to be determined. It is convenient to assign a post capacitance $C_p \equiv B_p / \omega$ and a whisker inductance $L_s \equiv X_s / \omega$ to replace B_p and X_s , although it is not known in advance whether C_p and L_s will be found to be positive and independent of frequency. (In analyses we have performed, C_p is usually positive, small, and varies with frequency; L_s is always positive and usually increases with frequency.)

If the mount is not symmetric and/or the signal source is not well matched, the generator impedance Y_g is complex. However, its imaginary part cannot be distinguished from post reactance, and can be treated as part of it. The real part of Y_g then constitutes a fourth unknown of the coupling network.

It is sometimes convenient to think of the network of Fig. 4(a) as a two port described by matrix $[y]$, shown in Fig. 4(b). This two port is determined by six real numbers (real and imaginary parts of $[y]$ matrix elements), as is the equivalent circuit of Fig. 4(a) ($C_p + n^2 \text{Im}Y_g$, R_s , L_s , C_d , n , $\text{Re}Y_g$). The following relations exist:

$$g_{11} = \text{Re}Y_g + \frac{R_s}{n^2 \{ (R_s^2 + (\omega L_s)^2 \}}$$

$$b_{11} = \frac{1}{n^2} \left(\omega C_p - \frac{\omega L_s}{(\omega L_s)^2 + R_s^2} \right) + I m Y_g$$

$$\begin{aligned}
g_{12} &= \frac{-R_s}{n\{R_s^2 + (\omega L_s)^2\}} \\
b_{12} &= \frac{\omega L_s}{n\{R_s^2 + (\omega L_s)^2\}} \\
g_{22} &= -g_{12}n \\
b_{22} &= \omega C_d - \frac{\omega L_s}{R_s^2 + (\omega L_s)^2}
\end{aligned}
\tag{10}$$

The experimental procedure consists of measuring the DC current change, ΔI , due to RF signal as a function of backshort position, l , and for a fixed DC bias voltage, V_B , which gives DC bias current I_B for zero RF signal. For acceptable accuracy without correction through (8) $\Delta I/I_B$ must be kept ≤ 0.1 . Since I_B is temperature dependent, drifts of $\Delta I/I_B$ of the order of .005 are typical and the modulated RF source system shown in Fig. 5 is convenient and more accurate; maximum $\Delta I/I_B$ of .01 can be used and the temperature drift of I_B has negligible effect.

The relation of a ΔI vs. l curve to the circuit element values can be easily found* by noting that ΔI is proportional to the square of the magnitude of the voltage across g_d (i.e., the power absorbed by g_d). Since all voltages in the network are proportional, ΔI is also proportional to the square of the magnitude of the input voltage at plane A - A of Fig. 4. Thus, we may write:

$$\Delta I = \frac{c|i_G|^2}{|Y_{IN} + Y_g + Y_{BS}|^2}$$

*We thank John Granlund for his contribution to the solution of this problem.

where i_G and Y_{IN} are defined in Fig. 4, and c is an arbitrary constant. Denoting jB_o as the value of Y_{BS} when ΔI is a maximum, and $j(B_o \pm \Delta B)$ as the values of Y_{BS} which give 1/2 the maximum ΔI , it is easily shown that:

$$Y_{IN} + Y_g = \Delta B - jB_o \quad (12)$$

Thus measuring two points on the ΔI vs. backshort position curve is equivalent to measuring the complex input admittance, Y_{IN} , which is related to the 6 unknowns (n , $C_p + n^2 \text{Im} Y_g$, $R_e Y_g$, R_s , L_s and C_d) and known diode conductance, g_d , by

$$Y_{in} = n^{-2} \left[j\omega C_p + \frac{j\omega C_d + g_d}{1 + (j\omega C_d + g_d)(R_s + j\omega L_s)} \right] - Y_g \quad (13)$$

Referring to Fig. 4(b), the same relation can be written as:

$$\Delta B - jB_o = y_{11} - \frac{(y_{12})^2}{y_{22} + g_d} \quad (14)$$

where $y_{mn} = g_{mn} + jb_{mn}$. The relation between the $[y]$ matrix elements and circuit parameters are then given by (10).

The diode conductance, g_d , can be varied over a wide range by varying the bias current, I_B , and thus, Y_{IN} can be determined (producing 2 real equations) for many values of g_d . However, each time I_B is changed, the diode capacitance, C_d , also changes, introducing one new variable. This is equivalent to changing the imaginary part of y_{22} every time a measurement is made. Thus, the measurement at each diode bias can be described by the equation:

$$\Delta B^{(k)} - jB_o^{(k)} = y_{11} - \frac{(y_{12})^2}{jb_{22}^{(k)} + g_{22} + g_d^{(k)}} \quad (15)$$

This equation can be rewritten in the form:

$$g_d^{(k)} + jB_{22}^{(k)} + g_{22} = \frac{(y_{12})^2}{y_{11} - \Delta B^{(k)} + jB_o^{(k)}} \quad (16)$$

Equating real and imaginary part of both sides, we get:

$$g_d^{(k)} = \text{Re} \left\{ \frac{(y_{12})^2}{y_{11} - \Delta B^{(k)} + jB_o^{(k)}} \right\} - g_{22} \quad (17)$$

$$b_{22}^{(k)} = \text{Im} \left\{ \frac{(y_{12})^2}{y_{11} - \Delta B^{(k)} + jB_o^{(k)}} \right\} \quad (18)$$

Equation (17) has 5 unknowns (g_{11} , b_{11} , g_{12} , b_{12} , g_{22}), therefore, at least 5 measurements must be made to determine them. Then unknown values of $b_{22}^{(k)}$, for every diode bias, can be found explicitly from (18). The circuit element values can then be found thru (10).

The solution of 5 or more (for reason of accuracy) real equations of the form (17), or 5 or more complex equations of the form (16) is not a simple task, since the equations are non-linear. It can be performed by utilizing numerical techniques on a digital computer, or thru an optimization program such as Compact [11]. An error sensitivity analysis could also be performed with either of these methods.

Our present approach has been not to solve for the ten unknowns directly, but to use other information and special characteristics of the equations to simplify the problem. An example of this approach will be given in the next section. Some of the possible simplifications are listed below:

1) For $I_B^{(1)} \sim 5 \text{ mA}$, $g_d^{(1)} \gg \omega C^{(1)}$ for most practical cases; $C_D^{(1)}$ has negligible effect upon $Y_{IN}^{(1)}$, and need not be determined.

2) The functional form of C_d , as a function of I_B (or V_B), may be known, and thus, all $C_d^{(k)}$ may be replaced by 2 unknowns, such as zero bias capacitance and barrier potential.

3) R_s may be known or predictable from low frequency measurements.

4) L_s , C_p , or n may be known from measurements on another diode at the same frequency.

5) $C_D^{(k)}$ may be known from measurements on the same diode at another frequency.

6) The mount may be assumed to be symmetric, and the signal source perfectly matched, then $Y_g = Z_G^{-1}$.

7) The obstacles (chip and whisker post) within the waveguide are small enough so C_p is negligibly small.

V. EXAMPLE OF 2-MM MIXER ANALYSIS

A. Evaluation Of A Diode Embedding Circuit

Two 140-220 GHz mixer mounts, designated A and B, were constructed using the design described by Kerr, et al, [9] and were equipped with diodes supplied by R. J. Mattauch of the University of Virginia. Scanning electron microscope photographs of the mounts are shown in Fig. 6(a), and 6(b), respectively. The diode chips have an array of platinum-gold

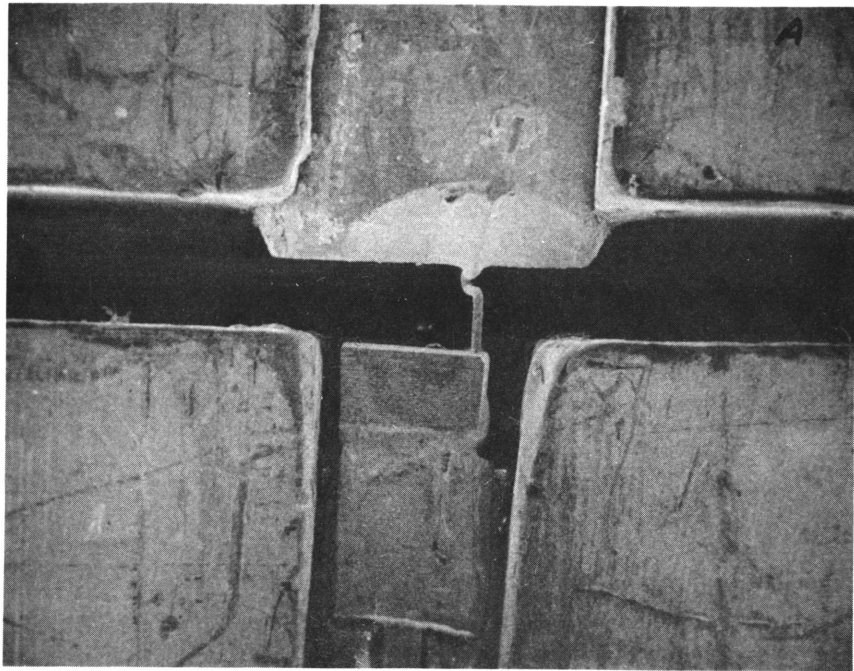


Fig. 6. Electron microscope photographs of the 2-mm mixer mounts: top is mixer A; bottom is mixer B.

anodes, 2 μm in diameter, fabricated by electroplating on lightly doped ($N_D \approx 4.5 \times 10^{16} \text{ cm}^{-3}$) epitaxial GaAs. Although the chips for mixers A and B came from the same wafer, they have undergone different processes of thinning of the epitaxial layer, resulting in slightly different diode geometry. The schematic cross section (not to scale) of the diodes in mount A and B is shown in Fig. 7.

These mounts were measured with the apparatus shown in Fig. 5 at a frequency of 152.8 GHz, and for the following diode bias currents: 5 mA, 1 mA, 500 μA , 200 μA , 50 μA , 20 μA , 5 μA .

The values of $\Delta B^{(k)}$ and $B_o^{(k)}$ for every current were determined as mean values of several analyses of the ΔI curve at different levels (typically 1, 2, 3 dB below peak).

The numerical procedure of finding circuit elements was based on the assumption that the mount is symmetric, and the source is well matched to the waveguide. Also, the high current approximation mentioned in the previous section was employed. That is, for $I_B^{(1)} = 5 \text{ mA}$, $g_d^{(1)} \gg \omega C_d$, and (12) and (13) reduce to:

$$B_o^{(1)} = n^{-2} \left\{ \frac{\omega L_s}{(\omega L_s)^2 + R_T^2} - \omega C_p \right\} \quad (19)$$

$$\Delta B_o^{(1)} = n^{-2} \left\{ \frac{R_T}{(\omega L_s)^2 + R_T^2} \right\} - Y_G \quad (20)$$

where $R_T = R_S + \frac{1}{g_d}$.

Equations (19) and (20), together with 2 equations of the form given by (17), can be solved for n , L_s , C_p , and R_s . However, it was recognized

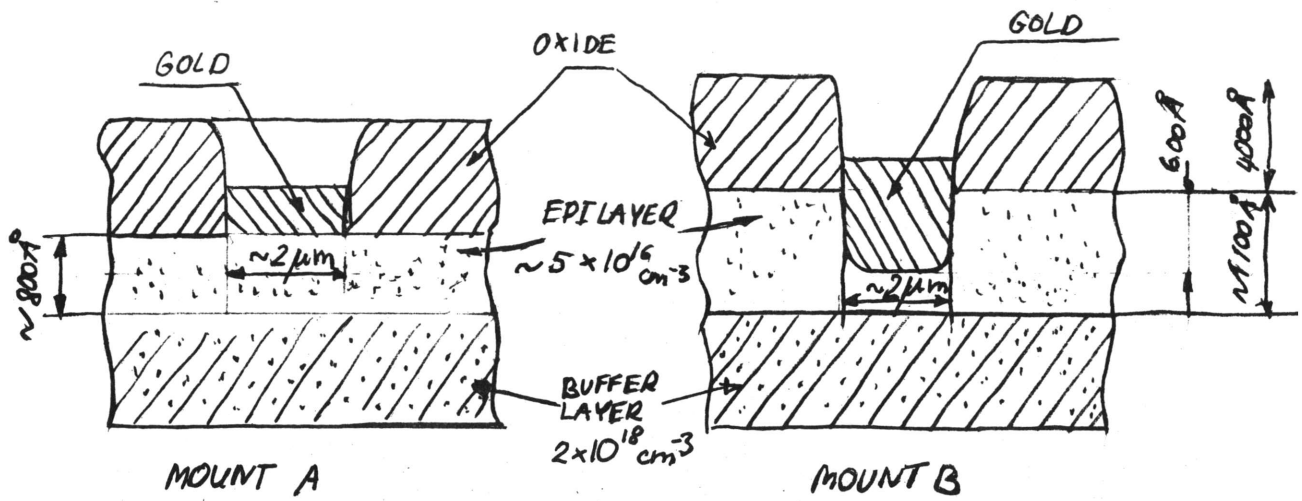


Fig. 7. The geometry of the Schottky-barrier diodes.

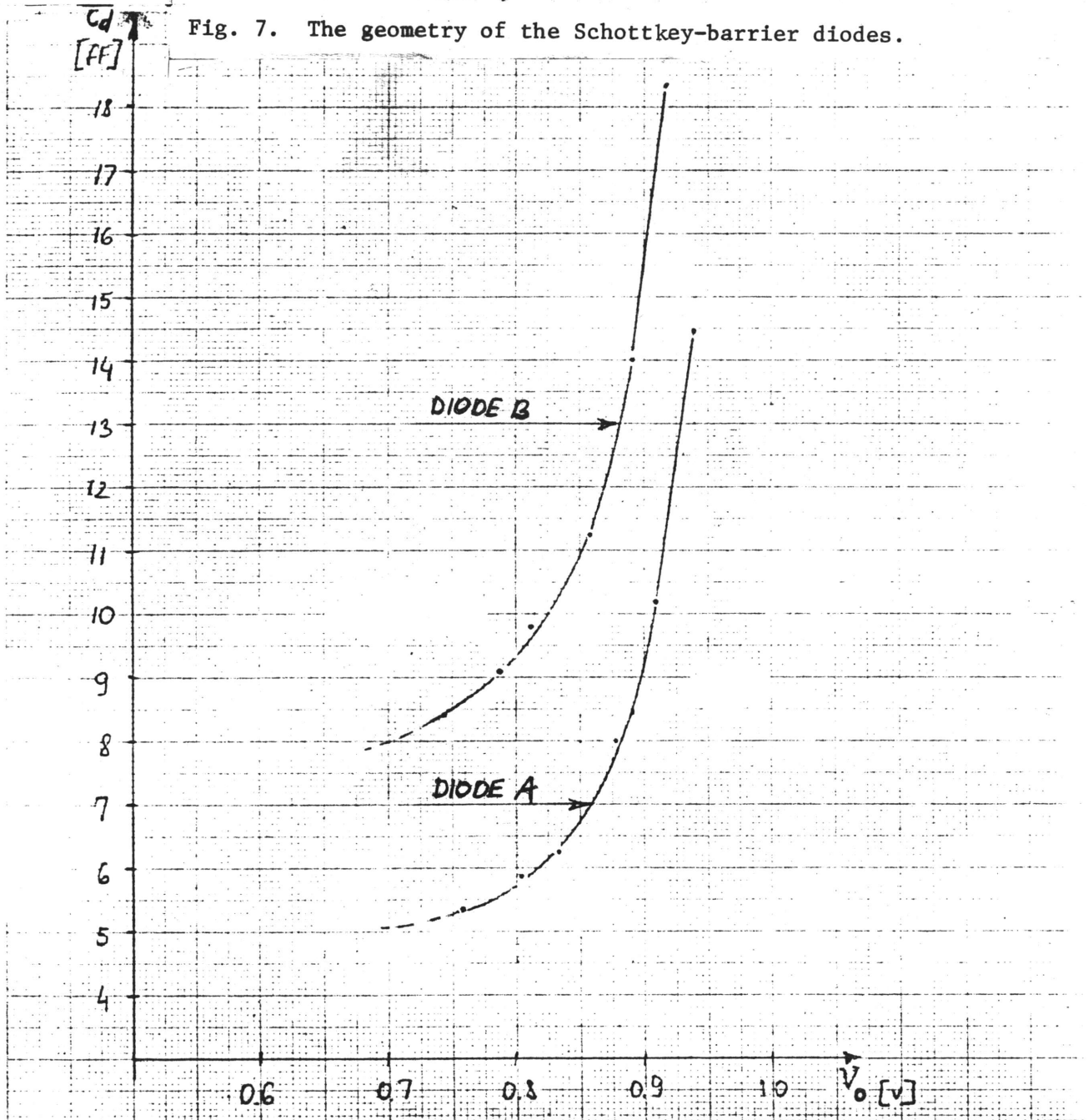


Fig. 8. The dependence of the diode capacitance C_d on the diode bias voltage V_0 .

that the value of the transformer turn ratio, n , is primarily determined by (20). This led to the following algorithm:

1) For the assumed value of n (usually $n \sim 1$), equation (19), together with 2 equations of the form (17) taken for 2 different bias currents, $I_o^{(2)}$ and $I_o^{(3)}$, was solved for L_s , C_p , and R_s . Capacitances $C_d^{(2)}$ and $C_d^{(3)}$ could then be found from (18). This was done for all fifteen pairs of possible $I_B^{(2)}$ and $I_B^{(3)}$ selected from the 6 remaining measurements. The solution of these equations was performed numerically on a Hewlett Packard 9830A desk-top computer, using the Newton-Raphson method [12]; typical computation time for one solution was fifteen seconds.

2) The mean values of L_s and R_s , from the fifteen solutions, were computed and used to find a new value of n from (20).

3) Steps 1 and 2 were repeated until 2 digit agreement for the value of n had been achieved in 2 consecutive iterations.

The results of this procedure are summarized in Table I for both mounts A and B. The mean values and standard deviation of C_p , L_s , R_s , and $C_d^{(k)}$ are given (as evident from the algorithm just described, the measurement resulted in fifteen values of C_p , L_s , R_s and 5 values of every $C_d^{(k)}$). For comparison, the results of some dc and low frequency measurements are also included.

A comparison of the results for mounts A and B shows different results for L_s , C_p , and n , as would be expected for the different geometry shown in Fig. 6. The whisker inductance has changed only a small amount, as the length of whisker wire was the same in both mounts (it was only bent differently).

MOUNT	DIODE IDEALITY FACTOR	R_s AT DC [Ω]	R_s AT 10MHz [Ω]	MEASURED AT 152.8 GHz									
				DIODE CAPACITANCE $C_d^{(*)}$ [fF]					R_s [Ω]	L_s [nH]	C_p [fF]	m	
				5 μ A	20 μ A	50 μ A	200 μ A	500 μ A					1 mA
A	1.15	14.7	17.0	5.3 (0.1)	5.9 (0.1)	6.2 (0.1)	8.0 (0.3)	10.2 (0.5)	14.5 (0.6)	24.9 (2.2)	0.110 (0.002)	6.6 (0.2)	0.90
B	1.15	10.1	12.0	8.4 (0.3)	9.1 (0.4)	9.8 (0.3)	11.2 (0.4)	14.0 (0.2)	18.3 (0.4)	25.1 (1.2)	0.129 (0.004)	2.0 (0.2)	0.82

NOTE: VALUES GIVEN IN BRACKETS ARE STANDARD DEVIATIONS (SEE TEXT)

Table I. The measured parameters of the diode and its embedding circuit.

The dependence of the diode capacitance C_d versus bias voltage V_B is shown in Fig. 8. The diode in mount A has considerably less capacitance than the diode in mount B. To check the consistency of the results, the curves $\frac{1}{C_d} = f(V_B)$ have been plotted in Fig. 9. These curves can be approximated by straight lines with slopes corresponding to doping concentrations of $N_D^A = 6.8 \times 10^{16} \text{ cm}^{-3}$ and $N_D^B = 1.9 \times 10^{17} \text{ cm}^{-3}$ for diodes A and B, respectively. In these computations the diameter of the diodes was assumed to be $2 \mu\text{m}$ and fringing effects were neglected. The epitaxial doping density measured by the manufacturer was $4.5 \times 10^{16} \text{ cm}^{-3}$. Higher doping is to be expected for diode B, since its epitaxial layer has been thinned more than diode A, and the depletion layer is closer to the highly doped ($N_D = 2 \times 10^{18} \text{ cm}^{-3}$) buffer layer.

The value of series resistance R_s is considerably higher than that expected from the diode chip alone. The skin effect at 150 GHz in the diode chip should add only about 3Ω to the diode resistance measured at 10 MHz [4][5]. This falls several ohms short of the measured values of R_s . The discrepancy is probably due to losses in the mount, choke, and whisker. However, it should be remembered that the mount equivalent circuit is for a lossless mount, and representation of mount losses as an effective increase in R_s is only an approximation.

Fig. 10 shows the $\Delta I = f(Y_{BS})$ curves for mixer A computed using values of circuit elements from Table I. Experimental points for each curve are also shown. As the agreement is excellent, it shows that the computational procedure adopted here was adequate.

10 X 10 TO THE CENTIMETER

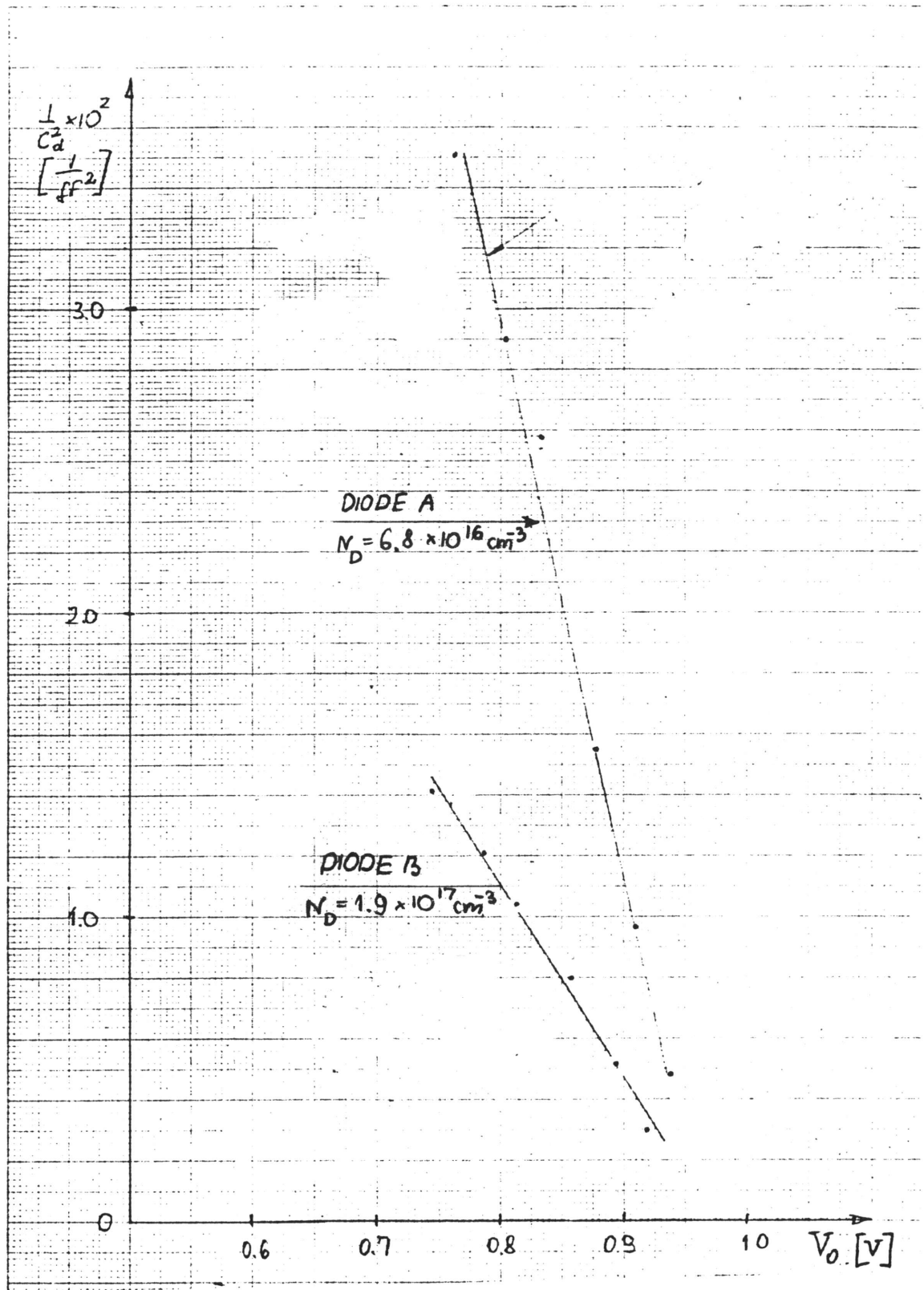


Fig. 9. The dependence of $\frac{1}{C_d^2}$ on the diode bias voltage V_0 .

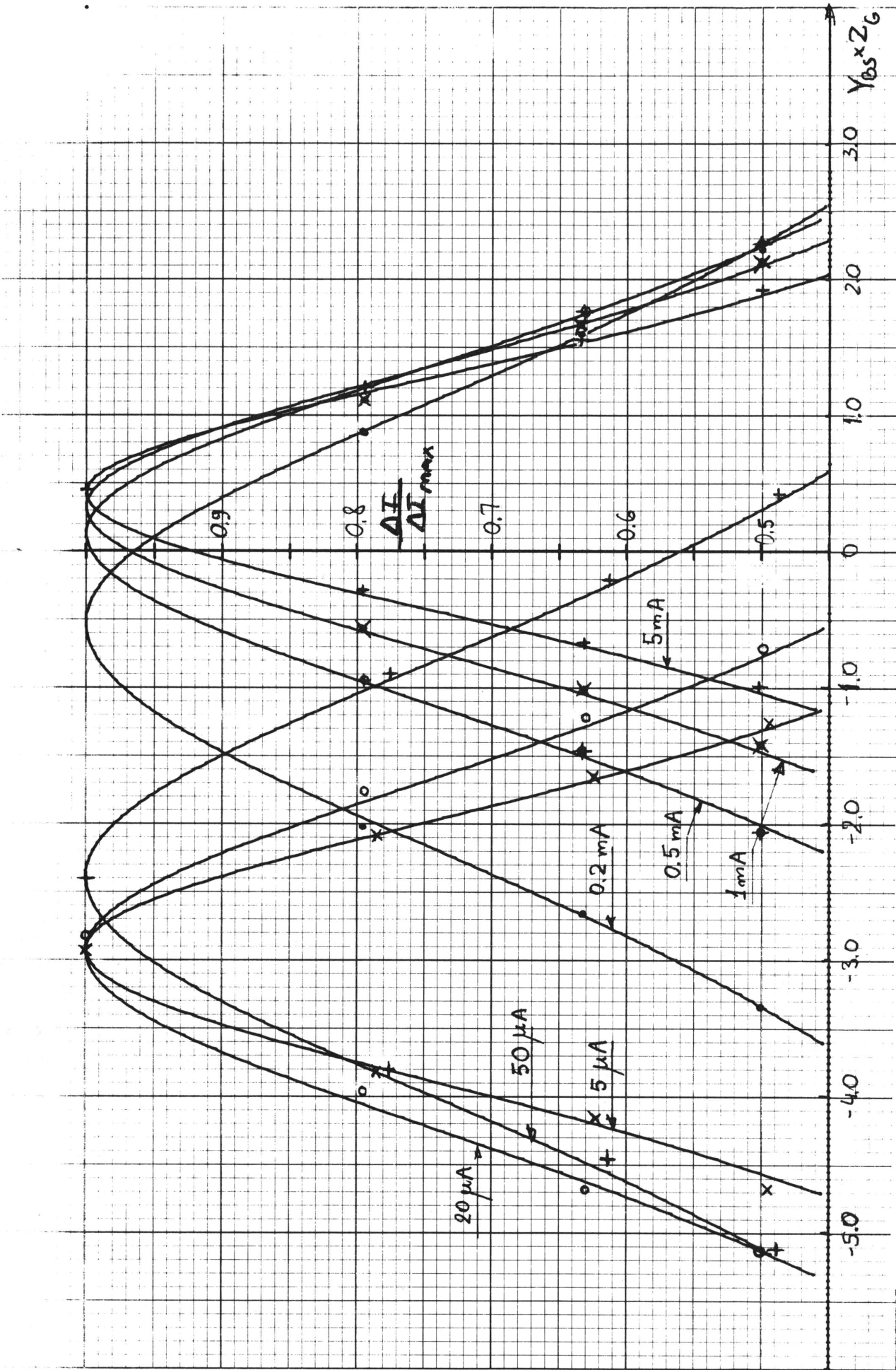


Fig. 10. The curves of $\frac{\Delta I}{\Delta I_{max}} = f(Y_{BS} \times Z_G)$ for mixer A computed using values of circuit elements from

Table I. Experimental points denoted were used to determine $\Delta B(k)$ and $\Delta B_0(k)$.

B. Embedding Network and Mixer Performance

The mixers were measured using a 4.75 GHz IF radiometer/reflectometer apparatus described by Weinreb and Kerr [13]. Table II summarizes the SSB performance of the room temperature mixers at 2 operating points corresponding to the best noise temperature T_{MXR} and best conversion loss L.

To explain the difference in the conversion loss of both mixers, the equivalent circuits determined previously were used to compute minimum loss, Δl , with respect to the backshort position, caused by the diode embedding circuit for different values of small signal resistances R_{RF} presented by the pumped diode (the capacitances for $V_B = 0.7V$ were assumed). The results of computations are presented in Fig. 11. The loss component due to reflection ΔL_R has been extracted from the total loss ΔL and is also plotted in Fig. 11.

As the resistance presented by the pumped diode at IF frequency R_{IF} was approximately 200Ω for both mixers, R_{RF} should be in the range 100 to 600Ω [14]. A particular value of R_{RF} , which would account for the 0.5 - 0.6 dB difference in the conversion loss of mixers A and B (compare Table II), is approximately 135Ω . This is in agreement with the common belief that a Y-type mixer [16] for which $R_{RF} \approx \frac{R_{IF}}{2}$ most closely describes the performance of millimeter-wave mixers.

VI. ERRORS

The previous example shows that very reasonable results can be obtained by the described method. However, application of this same method to the same mixer measured at 200 GHz gives poor results in that the iteration

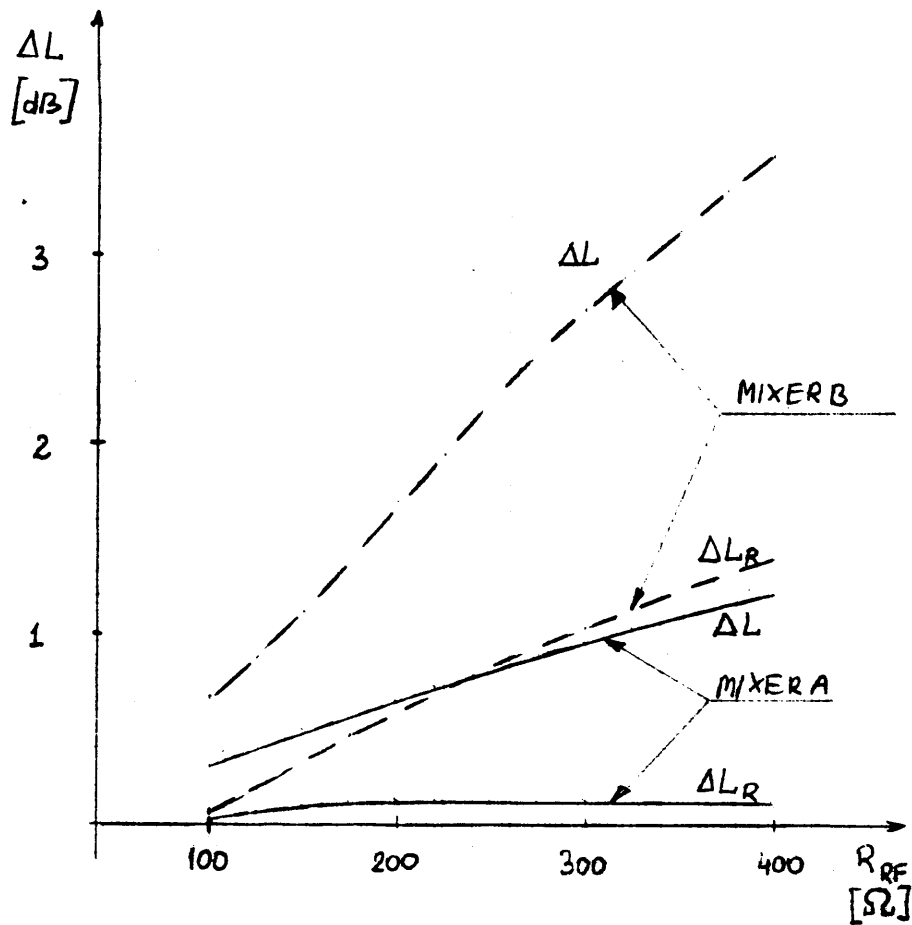


Fig. 11. The total loss ΔL and loss due to the reflection ΔL_R caused by the embedding circuits of mixers A and B versus resistance R_{RF} presented to the circuit by the pumped diode.

MIXER	BEST NOISE TEMPERATURE				BEST CONVERSION LOSS			
	V_o [V]	I_D [mA]	T_{mxx} [°K]	L [dB]	V_o [V]	I_D [mA]	T_{mnr} [°K]	L [dB]
A	0.70	0.70	850	6.75	0.3	2.0	1240	6.00
B	0.74	1.10	990	7.30	0.3	3.0	1560	6.65

Table II. The SSB performance of mixers ($f_p = 152.8$ GHz, $f_{IF} = 4.75$ GHz.)

procedure does not converge, and unreasonable element values are computed. This problem is being investigated further. Our present belief is that some of the problem is due to the computation procedure as will be discussed below, and this can be improved. It appears that the final result will be a method which: a) gives good accuracy ($\pm 10\%$ for element values) for some mounts, b) includes an error sensitivity computation procedure which gives the element error for a given measurement error, and c) allows good accuracy for all reasonable mounts if one of the element values is known by some other method.

The errors can be categorized into five areas which are discussed below: a) measurement error, b) errors due to invalid assumptions, c) computation convergence, d) error multiplication effecting y-parameters and element values, and e) error multiplication effecting only the element values.

A. Measurement Errors

With fairly conventional instrumentation, ΔI can be measured to within 1% of ΔI_{\max} . The errors due to backshort position readout have a larger effect for millimeter wave mounts. A typical good readout accuracy of .01 mm (i.e., ~ 0.5 mils) represents $\lambda_g/200$ at $\lambda_g = 2$ mm. The effect of this error on a given B and ΔB can be easily computed, and a computed sensitivity table for a given mount will allow determination of element value errors.

B. Validity of Assumptions

The two assumptions which have the most effect upon error are matched generator admittance ($Y_g = Y_G$) and mount symmetry; these have similar

effects. As discussed in IV, the first assumption need not be made, $\text{Re } Y_g$ can be determined by the computation procedure and $\text{Im } Y_g$ can be absorbed as part of C_p . However, to ease computation, we assumed $Y_g = Y_G$ for the example in V. It can be shown that a small source VSWR has the approximate effect of adding $\frac{1}{2} (\text{VSWR} - 1) Y_G$ to ΔB , where the VSWR includes the waveguide-height transformer. For the example of the previous section, a VSWR = 1.1 changes the computed value of n from 0.90 to 0.85 or 0.95. The effect upon the value of C_d , and other element values, is shown in Fig. 12 and Table III.

Mounts will be asymmetric if the diode whisker bend is in the direction of propagation (it need not be), and due to small fabrication differences very close to the diode. This problem has not been investigated, but it is believed that the effects will be small, since the departures from symmetry are usually small compared to a wavelength.

C. Computation Convergence Error

A closed form solution for y parameters or element values has not been found. These have been computed, using a successive approximation procedure which often does not converge. The lack of convergence is probably due to the effect of errors in the data. However, it is believed that an improved computation algorithm will alleviate this problem. All computation thus far has been performed on a HP 9830 calculator, and a faster computer would make using a larger data set feasible, including a model of diode capacitance variation, and a more sophisticated computation scheme.

D. Error Multiplication Effecting $[y]$ Parameters and Element Values

It is fundamental to all methods of determining a network by

[pF]

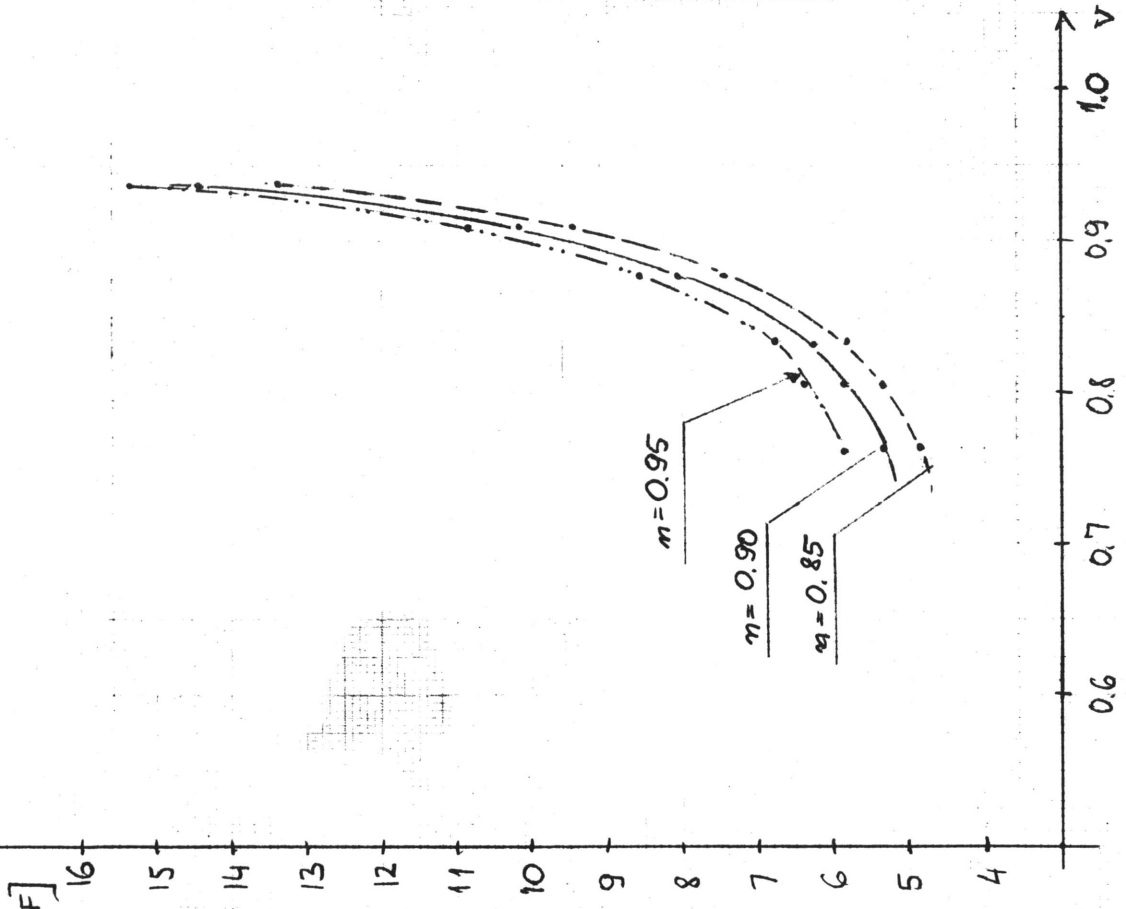


Fig. 12

TABLE III

n	C_d [pF]	R_s [Ω]	L_s [nH]	C_d at 0.8V
0.90	6.6 ± 0.2	24.9 ± 2.1	0.110 ± 0.02	5.9 ± 0.1
0.85	6.3 ± 0.2	28.2 ± 3.7	0.118 ± 0.03	5.4 ± 0.1
0.95	7.0 ± 0.2	22.0 ± 1.6	0.104 ± 0.002	6.4 ± 0.1

Fig. 12 and Table III. Measured diode capacitance for a 2 mm mixer mount as a function of bias voltage for various values of turns ratio, n . The determined value of $n = 0.9$, but a source VSWR of 1.10 could change this to 0.85 or 0.95, dependent on phase. The effect on other element values is shown in Table III.

measuring the impedance at one port with a variable load at the other port, that the method breaks down as $y_{12}y_{21}$ becomes small. The method described in this paper certainly falls in this category. As the diode becomes decoupled from the input waveguide (by L_s or C_d becoming large), less effect on B and ΔB will be measured as the bias current is varied and less information is determined about the network. Larger errors in both $[y]$ parameters and element values will result for a given error in B and ΔB . Fortunately, this is not the case for an efficient diode mount, whether its purpose be for mixing, detection, frequency multiplication, or power control. Conversely, if a mount shows little variation in B or ΔB with bias current, it may be assumed that the mount is inefficient without further analysis.

E. Error Multiplication Effecting Element Values Only

It can easily be shown that the element values in the equivalent circuit are not unique when $R_s = 0$. (The transformer turns ratio, n , can be varied and this can be compensated for by different values in the Π -network consisting of C_p , L_s , and C_d .) Thus, large errors in element values, but not in circuit $[y]$ parameters, should be expected for small values of R_s (more precisely, for $R_s \ll (L_s\omega)^2/Z_G$). This tends to be the case for an efficient diode. However, the power transfer properties of the coupling network can still be computed from the $[y]$ parameters. Furthermore, if one element of n , C_p , L_s , or C_d is known by some other method then the other elements can be found even if $R_s = 0$.

REFERENCES

- [1] R.L. Eisenhart, P.J. Kahn, "Theoretical and experimental analysis of waveguide mounting structure," IEEE Trans. Microwave Theory Tech., vol. MTT-19, pp. 706-720, 1971.
- [2] J.S. Joshi, J.A.F. Cornic, "Analysis of waveguide post configurations," IEEE Trans. Microwave Theory Tech., vol. MTT-25, pp. 169-183, 1977.
- [3] B.C. DeLoach, "A new microwave measurement technique to characterize diodes and an 800-GC cutoff frequency varactor at zero volts bias," IEEE Trans. Microwave Theory Tech., vol. MTT-12, pp. 15-20, 1964.
- [4] D.N. Held, A.R. Kerr, "Conversion loss and noise of microwave and millimeter-wave mixers: Part 2 - Experiment," IEEE Trans. Microwave Theory Tech., vol. MTT-26, pp. 55-61, 1978.
- [5] D.N. Held, "Analysis of room temperature millimeter wave mixers using GaAs Schottley barrier diodes," Sc. D. Dissertation, Dept. of Electrical Engineering, Columbia University, New York, 1976.
- [6] C.E. Hagström, E.L. Kollberg, "A method for measuring embedding impedance of diode mounts applied to millimeter-wave mixers." Research Laboratory of Electronics and Onsala Space Observatory Res. Rep. No. 135, Gothenburg, Sweden, 1979.
- [7] A.R. Kerr, R.J. Mattauch, J.A. Grange, "A new mixer design for 140-220 GHz mixer," IEEE Trans. Microwave Theory Tech., vol. MTT-25, pp. 399-401, 1977.
- [8] C.G. Montgomery, R.H. Dicke, E.M. Purcell, "Principles of microwave circuits," McGraw-Hill Book Company, New York, 1948.
- [9] M. Sucher, J. Fox, "Handbook of microwave measurement," vol. 1, Polytechnic Press of the Polytechnic Institute of Brooklyn, New York, 1963.
- [10] A.M. Cowley, H.O. Sorenson, "Quantitative comparison of solid-state microwave detectors," IEEE Trans. Microwave Theory Tech., vol. MTT-14, pp. 588-602, 1966.
- [11] COMPACT, "Computerized optimization of microwave passive and active circuits," available from Compact Engineering, Inc., 1088 Valley View Court, Los Altos, Ca., 94022.
- [12] Reverence on Newton-Raphson method. Reference Data for Radio Engineers, Fifth Edition, H.W. Sams, 1970, p. 44-39.
- [13] S. Weinreb, A.R. Kerr, "Cryogenic cooling of mixers for millimeter and centimeter wavelength," IEEE J. Solid State Circuits, vol. SC-8, pp. 58-63, Feb. 1973.
- [14] A.A.M. Saleh, "Theory of Resistive Mixer," Cambridge, Mass., MIT Press, 1971.

APPENDIX 1.

SUMMARY OF EXPERIMENTAL DATA ON 2-mm MIXERS

This appendix contains results of detailed measurement on 2-mm mixers. Two mounts were investigated. Mount A (mount No. 2) and mount B (mount No. 3) have been assembled with 2P11 and 2P8-600 diode chips, respectively. The electron microscope photographs of both mounts and the schematic cross section of the diode chips have been shown in Figures 6 and 7.

A.1.1. D.C. and Low-Frequency Measurements

The d.c. characteristics of 2P11 and 2P8-600 diodes are shown in Fig. A.1. The shape of the curve for the 2P11 diode in its high current region suggests deviation from the normally assumed d.c. model composed of an ideal diode and a series resistance R_S . This is further confirmed by measurement of the small signal diode resistance R_T at a frequency of 10 MHz, which is shown in Fig. A.2. This resistance is equal to the sum of the series resistance R_S and the differential resistance of the diode $R_d = \frac{1}{g_d}$ and should therefore be a linear function of $(\frac{1}{I_D})$. Small deviations of the measured points from the straight line for the 2P11 diode are apparent, but they are not for the 2P8-600 diode. This effect is probably connected with the negative differential mobility of carriers in GaAs in high electric fields. The doping concentration of the 2P8-600 diode is three times that of the 2P11 diode. This may explain why a similar effect was not observed in the 2P8-600 diode.

This effect should be further investigated as it can be strongly dependent on frequency and diode physical temperature as well. Therefore it could be of importance in understanding the behavior of mm-wave cooled mixers.

A.1.2. The Backshort Measurements

Backshort measurements were performed using the measurement set-up shown

in Fig. 5 at frequencies of 152.8 GHz and 200.3 GHz. The maximum change of d.c current flowing through the diode due to the presence of the microwave signal was about 1%. Tables A.1. and A.2. summarize the data taken for mixers A and B, respectively. Each value of $\Delta B^{(k)}$ and $B_o^{(k)}$ was computed as the mean value of three results recovered from measurements at levels 1, 2, and 3 dB below the peak of the curve. The number given in parentheses is the standard deviation of these three results. The values of ΔV best describing the assumed exponential form of d.c. characteristic of the diode around the given operating point are also included.

Table A.3. shows the dependence of the signal power needed to produce $\frac{\Delta I_{\max}}{I_B} = 0.1$ on the diode bias at 152.8 GHz. The power levels given in the Table are computed relative to the power level at $I_B = 50\mu A$. Similar measurements were not performed at 200.3 GHz as the precise attenuator had not been available at this frequency.

A.1.3. Mixer Measurements

The noise temperature and conversion loss of both mixers have been measured at 152.8 and 201.3 GHz using the hot-cold load technique. The R.F. portion of the measuring set-up is schematically shown in Fig. A.3. for the two frequencies. The mixer parameters are summarized in Table A.4. The conversion loss L_{dB} and noise temperature T_{MXR} of Table A.3. have been corrected for the R.F. losses in front of the mixers that are indicated in Fig. A.3. and also for the reflection at the I.F. port. The modulus of the I.F. port reflection coefficient $|\Gamma_{IF}|$ given in Table A.3. was measured through the 50/200 Ω transformer. The measurements at the operating point for least conversion loss at 201.3 GHz have not been performed because of insufficient pump power from the doubler.

The pump power necessary to pump the mixers at 152.8 GHz at the operating

point where the least noise temperature has been observed, was about 0.25mW for mixer A and 0.35mW for mixer B. For mixer A at 201.3 GHz it was about 0.3mW. This power is measured by replacing the mixer mount with a power met

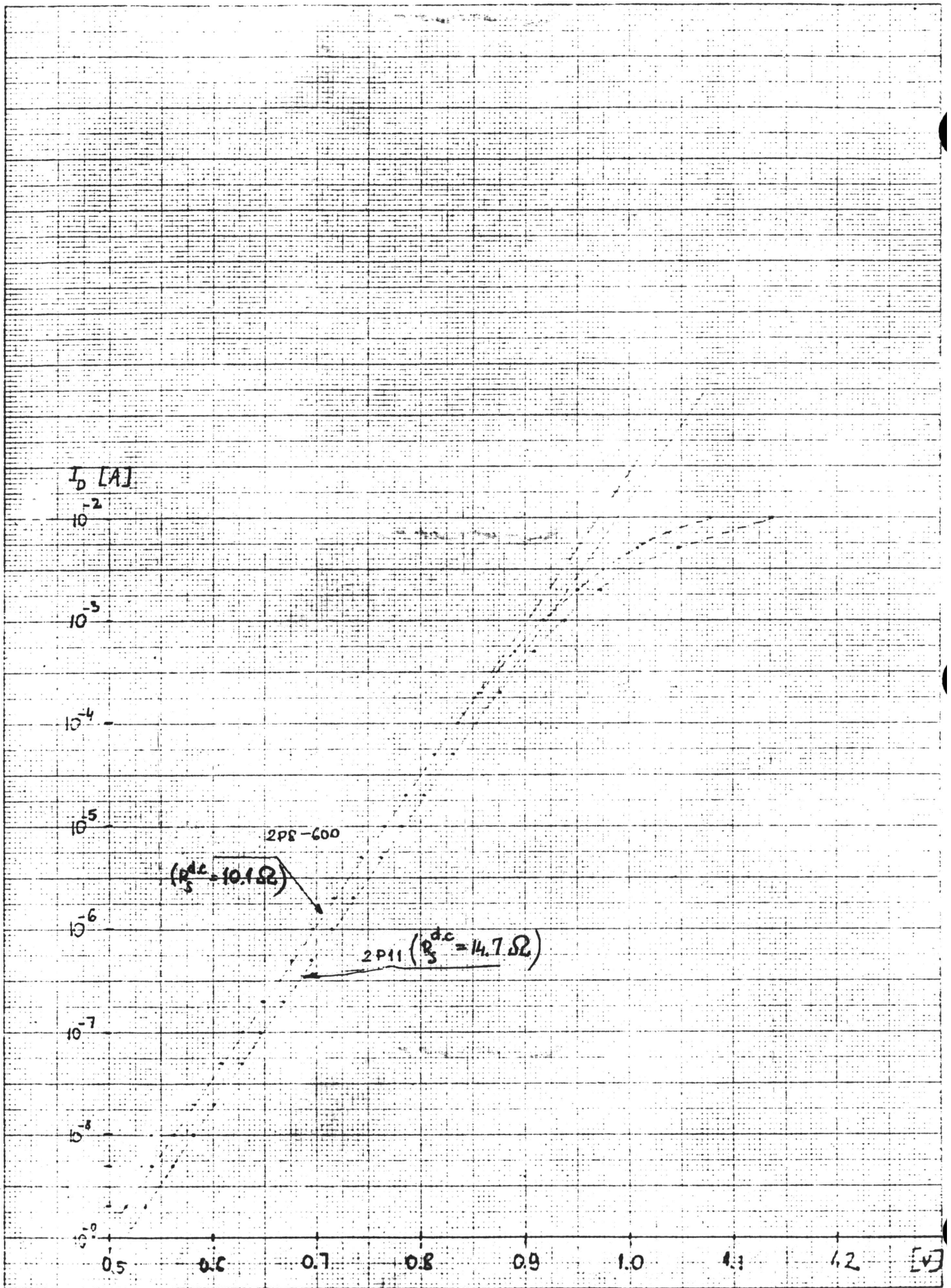


Fig. A.1. D.C. characteristics of the 2P11 and 2P8-600 diodes.

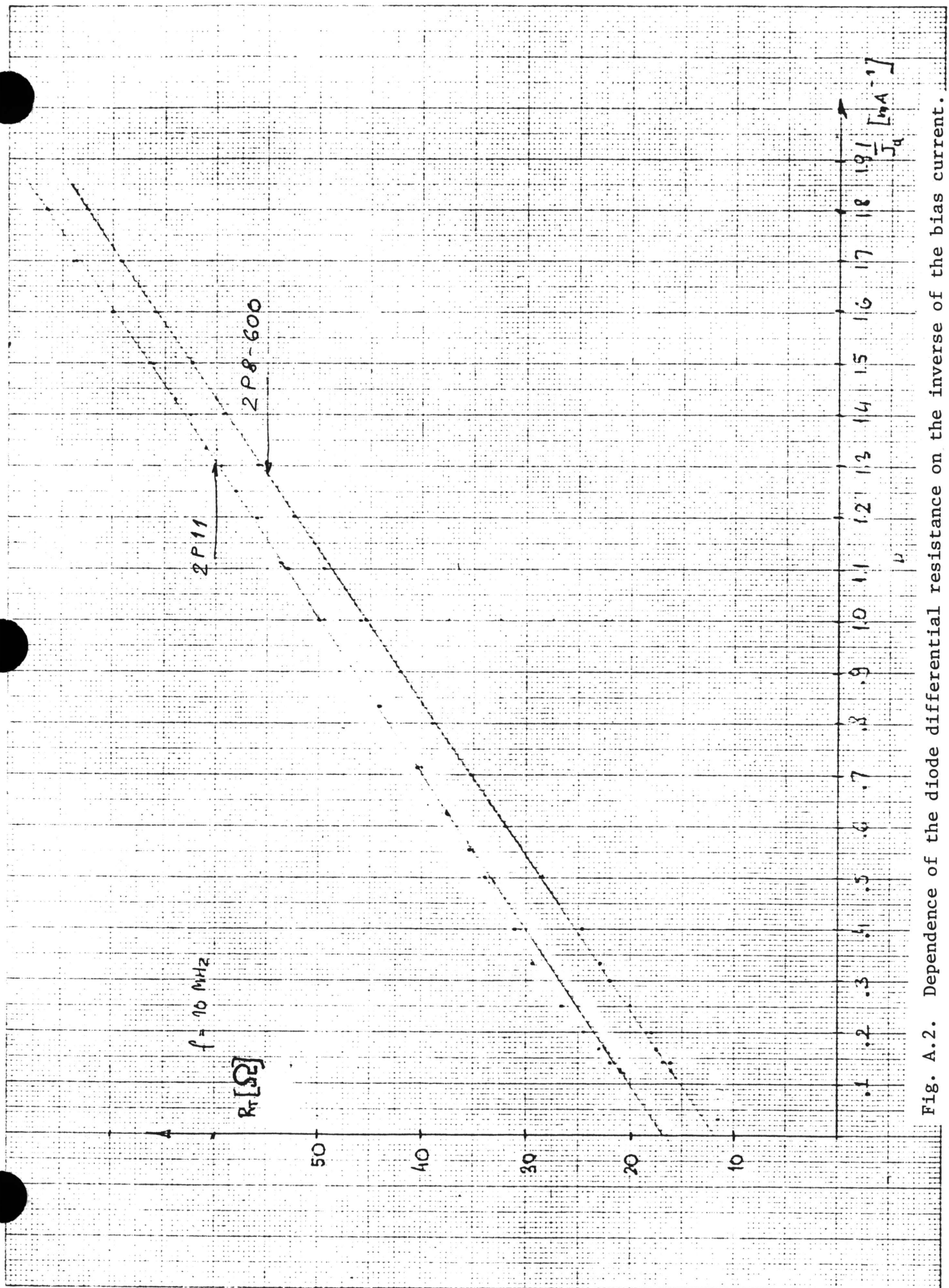


Fig. A.2. Dependence of the diode differential resistance on the inverse of the bias current.

TABLE A1

DIODE BIAS CURRENT I_D [mA]	ΔV [mV]	FREQUENCY			
		152.8 GHz		200.3 GHz	
		β_0	ΔB	β_0	ΔB
8	70.5	0.456 (0.028)	1.328 (0.02)	0.384 (0.008)	0.959 (0.018)
5	70.5	0.458 (0.006)	1.463 (0.011)	0.355 (0.006)	0.994 (0.006)
1	70.5	0.340 (0.015)	1.753 (0.013)	0.356 (0.009)	1.093 (0.018)
0.5	70.5	0.126 (0.034)	2.133 (0.017)	0.396 (0.006)	1.201 (0.004)
0.2	70.5	-0.564 (0.02)	2.809 (0.039)	0.582 (0.006)	1.446 (0.010)
0.05	69.4	-2.355 (0.035)	2.719 (0.039)	1.249 (0.035)	1.722 (0.027)
0.02	69.0	-2.918 (0.057)	2.221 (0.041)	1.633 (0.025)	1.728 (0.041)
0.005	67.9	-2.925 (0.033)	1.647 (0.045)	2.067 (0.016)	1.769 (0.020)

Table A.1. Summary of backshort measurements on mixer A at 152.8 and 200.3 GHz.

TABLE A 2

DIODE BIAS CURRENT I_D [mA]	ΔV [mV]	FREQUENCY			
		152.8 GHz		200.3 GHz	
		B_0	ΔB	B_0	ΔB
8	72.5	1.258 (0.025)	1.406 (0.019)	0.904 (0.017)	0.914 (0.017)
5	72.5	1.224 (0.032)	1.434 (0.011)	0.998 (0.011)	0.973 (0.016)
1	72.5	1.199 (0.028)	1.773 (0.045)	0.907 (0.013)	0.981 (0.029)
0.5	72.5	1.211 (0.028)	2.046 (0.072)	0.921 (0.025)	0.997 (0.010)
0.2	71.5	1.191 (0.047)	2.918 (0.097)	1.220 (0.022)	1.274 (0.043)
0.05	68.6	1.423 (0.022)	5.128 (0.027)	1.445 (0.025)	1.220 (0.020)
0.02	68.2	1.290 (0.05)	6.80 (0.1)	1.340 (0.014)	1.044 (0.034)
0.005	67.2	-0.09	8.89 (0.1)	1.362 (0.024)	0.947 (0.038)

Table A.2. Summary of backshort measurements on mixer B at 152.8 and 200.3 GHz.

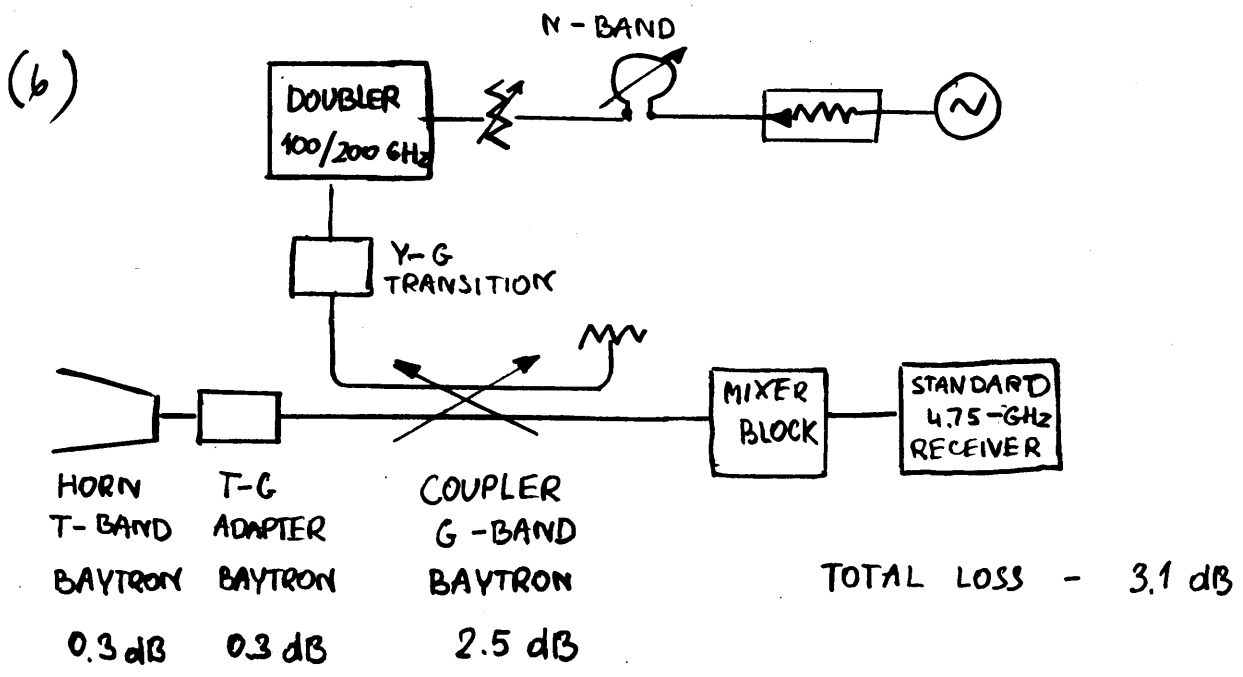
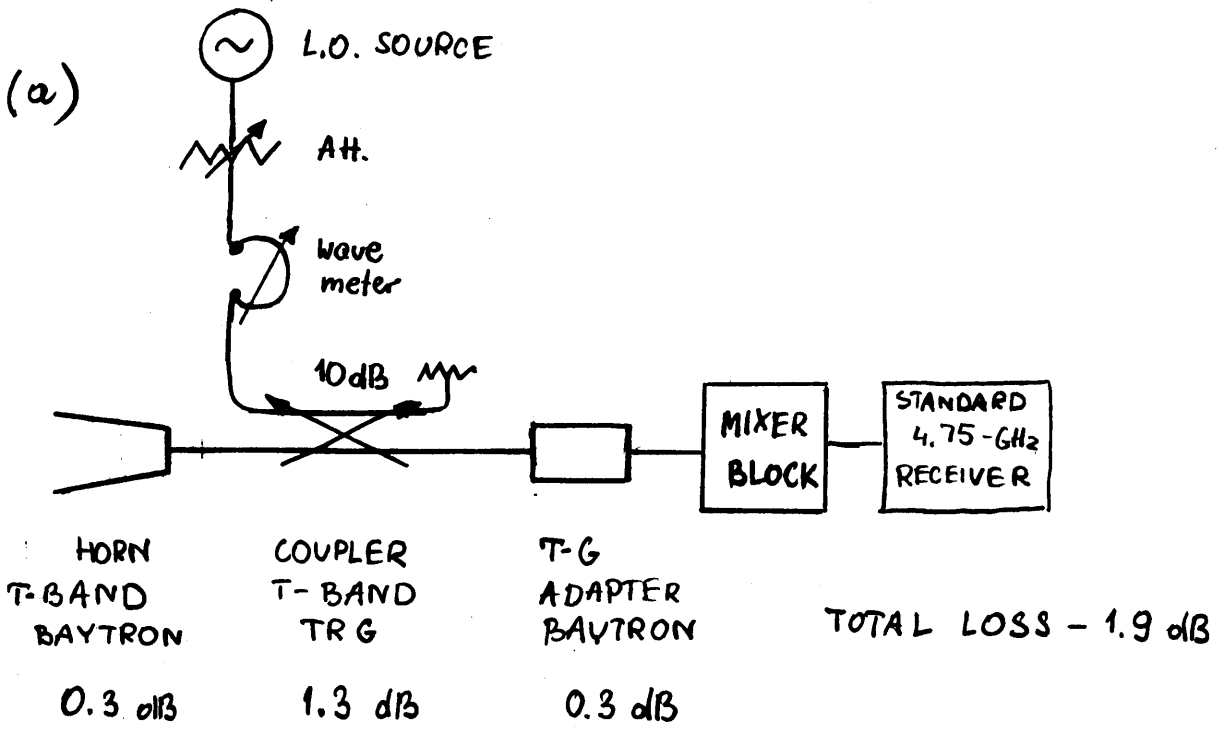


Fig. A.3. The conversion loss and noise temperature measurement set-up used at 152.8 GHz (a) and 201.3 GHz (b).

MIXER	DIODE DIAS			+B L[mA]
	500	200	50	
A	10.2	5.7	0	-3.1
B	7.6	3.4	0	-1

Power level [dB] -5.6 -1.8

Table A.3. The dependence of the signal level needed to produce $\frac{\Delta I_{\max}}{I_B} = 0.1$ at 152.8 GHz.

FREQUENCY [GHz]	MIXER					LEAST NOISE TEMPERATURE					LEAST CONVERSION LOSS				
	V _b [V]	I _p [mA]	T _{mixr} [°K]	L [dB]	Γ _{IF}	V _b [V]	I _p [mA]	T _{mixr} [°K]	L [dB]	Γ _{IF}	V _b [V]	I _p [mA]	T _{mixr} [°K]	L [dB]	Γ _{IF}
152.8	0.70	0.70	850	6.75	0.17	0.3	2.0	1240	6.00	0.23	0.3	2.0	1240	6.00	0.23
	0.74	1.10	990	7.30	0.16	0.3	3.0	1560	6.65	0.13	0.3	3.0	1560	6.65	0.13
201.3	0.74	0.74	865	6.95	0.10	0.3	2.0	1240	6.00	0.23	0.3	2.0	1240	6.00	0.23
	0.75	0.90	1830	9.10	0.11	0.3	3.0	1560	6.65	0.13	0.3	3.0	1560	6.65	0.13

Table A.4. Summary of 4.75 GHz IF₁ SSB mixer performance with pump at 152.8 and 200.3 GHz.

APPENDIX 2.

COMPUTER PROGRAMS FOR DIAGNOSIS OF MICROWAVE MIXER MOUNTS

The computer programs described in this appendix were written in BASIC for the H-P 9830A computer in connection with the development of the mixer mount measurement method described previously. These programs can be divided into two groups: programs that determine a mixer mount equivalent circuit from measured data, and programs which compute the parameters of a given equivalent circuit that are related to mixer performance.

A.2.1. Programs for Determining the Mixer Mount Equivalent Circuit

The equivalent circuit of the mixer mount used in these programs is shown in Fig.3. As was previously explained, to find the elements of the equivalent network of Fig.3 one has to solve a set of nonlinear equations of the general form

$$\Delta B^{(k)} - jB_o^{(k)} = y_{11} - \frac{(y_{12})^2}{jb_{22}^{(k)} + g_{22} + g_d^{(k)}} \quad (A.1)$$

where

$$g_{11} = \text{Re}Y_g + \frac{R_s}{n^2 \{R_s^2 + (\omega L_s)^2\}}$$
$$b_{11} = \frac{1}{n^2} \left(\omega C_p - \frac{\omega L_s}{(\omega L_s)^2 + R_s^2} \right) + \text{Im}Y_g$$
$$g_{12} = \frac{-R_s}{n \{R_s^2 + (\omega L_s)^2\}}$$
$$b_{12} = \frac{\omega L_s}{n \{R_s^2 + (\omega L_s)^2\}} \quad (A.2)$$

$$g_{22} = -g_{12}^n$$

$$b_{22} = \omega C_d - \frac{\omega L_s}{R_s^2 + (\omega L_s)^2}$$

and

$g_d^{(k)}$ - the differential conductance of the diode biased at $I_o^{(k)}$

η - the ideality factor of the diode

κ - Boltzmann's constant

τ - absolute temperature

$\Delta V = V_{01} - V_{02}$ satisfying $I_o(V_{01}) = 10 \times I_o(V_{02})$ and corrected for the effect of d-c series resistance

$B_o^{(k)}, \Delta B^{(k)}$ - the position of the maximum and the 3-dB bandwidth of the

$$\Delta I = f \left(\frac{Y_{BS}}{Y_G} \right) \text{ curve, respectively}$$

The set of equations having the general form of (A.1) can be solved in many different ways depending on what prior knowledge, if any, of the moun or diode parameters, is assumed.

Several programs solving this set are described in the following. Although different in details, the basic approach to the solution is the same for all of them. First, the set of equations is converted into a set of real equations. Then it is solved by the Newton-Raphson method, to be described next.

Given the set of equations

$$\begin{aligned} f_1(V_1, V_2, \dots, V_m) &= 0 \\ f_2(V_1, V_2, \dots, V_m) &= 0 \\ &\vdots \\ f_m(V_1, V_2, \dots, V_m) &= 0 \end{aligned} \tag{A.3}$$

one can present it in the matrix form

$$[f([V])] = [0] \quad (A.4)$$

where $[V]$ is the column matrix of m unknowns $V_1 \dots V_m$.

Some initial value of $[V]$ is taken, and every next approximation to the solution is computed using, successively, the formula:

$$[V]_{n+1} = [V]_n + [\Delta V] \quad (A.5)$$

where $[\Delta V]$ is the solution of the following matrix equation

$$[f([V]_n)] + [J([V]_n)] \times [\Delta V] = [0] \quad (A.6)$$

and $[J([V]_n)]$ is the Jacobian matrix of the form

$$[J([V])] = \begin{bmatrix} \frac{\delta f_1}{\delta V_1} & \frac{\delta f_1}{\delta V_2} & \dots & \frac{\delta f_1}{\delta V_m} \\ \vdots & \vdots & \vdots & \vdots \\ \frac{\delta f_m}{\delta V_1} & \dots & \dots & \frac{\delta f_m}{\delta V_m} \end{bmatrix} \quad (A.7)$$

and evaluated for $[V] = [V]_n$.

Therefore

$$[V]_{n+1} = [V]_n - [J([V]_n)]^{-1} \times [f([V]_n)] \quad (A.8)$$

It should be noted that, depending on the initial values of $[V]$ assumed, this method may not converge. Therefore, for the user's convenience, every program provides a printout of the quantity

$$E = \sqrt{|f_1|^2 + |f_2|^2 + \dots + |f_m|^2} \quad (A.9)$$

at every step.

Program in File 0

This program solves the set of four equations of the following form:

$$g_d^{(k)} = \operatorname{Re} \left[\frac{(y_{12})^2}{y_{11} - \Delta B^{(k)} + jB_o^{(k)}} \right] - g_{22} \quad (\text{A.10})$$

It is assumed that the signal source is perfectly well matched to the waveguide, and therefore $Y_g = Y_G$. Then only four equations are needed to find n, L_s, R_s, C_p .

The diode capacitances are found from the following relations:

$$\omega C_d^{(k)} = b_{22}^{(k)} + b_{12}' = \operatorname{Im} \left[\frac{(y_{12})^2}{y_{11} - \Delta B^{(k)} + jB_o^{(k)}} \right] + b_{12}' \quad (\text{A.11})$$

Equation (A.10) can be rewritten in the following form

$$\begin{aligned} & \left[g^2 - (b_{12}')^2 \right] \left[g - n^2(\Delta B^{(k)} - Y_G) \right] - 2b_{12}'g \left[b_{11}' + n^2B_o^{(k)} \right] \\ & - \left[g + g_d^{(k)} \right] \left[\left[g - n^2(\Delta B^{(k)} - Y_G) \right]^2 + \left[b_{11}' + n^2B_o^{(k)} \right]^2 \right] = 0 \end{aligned} \quad (\text{A.12})$$

$$\text{where } g = \frac{R_s}{R_s^2 + (\omega L_s)^2} \quad b_{12}' = \frac{\omega L_s}{R_s^2 + (\omega L_s)^2} \quad b_{11}' = \omega C_p - b_{12}' \quad (\text{A.13})$$

The corresponding form of equation (A.11) is

$$\omega C_d^{(k)} = \frac{-2gb_{12}' \left[g - n^2(\Delta B^{(k)} - Y_G) \right] - (g^2 - b_{12}'^2)(b_{11}' + n^2B_o^{(k)})}{\left[g - n^2(\Delta B^{(k)} - Y_G) \right]^2 + (b_{11}' + n^2B_o^{(k)})^2} + b_{12}' \quad (\text{A.14})$$

Equations (A.12) and (A.14) in their normalized form ($Y_G = 1$) were actually used in the program. The program listing and an example of the printout during execution are shown on the next pages.

It should be noted, however, that on some sets of input data this program did not converge well, or did not converge at all. It is possible that in the presence of measurement errors in the input data, the set of nonlinear equations does not have a solution.

In the printout example, the diode capacitance C_d for $I_B = 5\text{mA}$ takes an unreasonable value. This is caused by the fact that for high current, $g_d^{(k)}$ is extremely large, which leads to

$$g \approx n^2 (\Delta B - Y_G) \quad (\text{A.1})$$

$$b_{11}' \approx -n^2 B_0$$

and therefore the first term in Equation (A.14) is extremely sensitive to very small measurement errors.

WAVEGUIDE DIMENSIONS IN MILLS A= 51.0 B= 6.4
 FREQUENCY= 152.80GHZ
 CURRENT 1: I= 5.00000 MA DELTA V= 70.50 MV
 B0/Y10= 0.458 DELTA B/Y10= 1.467
 CURRENT 2: I= 0.50000 MA DELTA V= 70.50 MV
 B0/Y10= 0.126 DELTA B/Y10= 2.133
 CURRENT 3: I= 0.05000 MA DELTA V= 69.40 MV
 B0/Y10= -2.355 DELTA B/Y10= 2.719
 CURRENT 4: I= 0.00500 MA DELTA V= 67.90 MV
 B0/Y10= -2.925 DELTA B/Y10= 1.647
 INITIAL VALUES: WSKR. INDUCTANCE= 0.110 NH POST CAP.= 6.20
 RESISTANCE= 25.00 OHM TURNS RATIO= 0.90
 0.105682881
 0.017014052
 1.59821E-03
 2.46953E-05
 6.29114E-09
 FINAL VALUES: RESISTANCE= 27.08 OHM INDUCTANCE= 0.113 NH
 POST CAPACITANCE= 6.17 FF TURNS RATIO= 0.87
 DIODE CAPACITANCES:
 C= -60.42 FF FOR I= 5.00000 MA
 C= 8.71 FF FOR I= 0.50000 MA
 C= 5.95 FF FOR I= 0.05000 MA
 C= 5.12 FF FOR I= 0.00500 MA


```

10 DIM FC(4),JC(4),JC(4),JC(4),ZC(4),YC(4),GC(4),WC(4),IC(4),CC(4)
20 DISP "WAVEGUIDE DIMENSIONS IN MILLS: A,B;"
30 INPUT A,B
40 WRITE (15,90)A,B
50 DISP "FREQUENCY =";
60 INPUT F1
70 WRITE (15,80)F1
80 FORMAT "FREQUENCY=" ,F7.2,"GHZ"
90 FORMAT "WAVEGUIDE DIMENSIONS IN MILLS",5X,"A=" ,F5.1,4X,"B=" ,F5.1
100 DISP "CURRENT 1: I=" ,F8.5," MA",2X,"DELTA V=" ,F6.2," MV"
110 INPUT IC(1),WC(1),YC(1),ZC(1)
120 WRITE (15,130)IC(1),WC(1)
130 FORMAT "CURRENT 1: I=" ,F8.5," MA",2X,"DELTA V=" ,F6.2," MV"
140 WRITE (15,150)YC(1),ZC(1)
150 FORMAT 18X,"B0/Y10=" ,F8.3,2X,"DELTA B/Y10=" ,F8.3
160 DISP "CURRENT 2: I,DELTA V,B0,DELTA B=";
170 INPUT IC(2),WC(2),YC(2),ZC(2)
180 WRITE (15,190)IC(2),WC(2)
190 FORMAT "CURRENT 2: I=" ,F8.5," MA",2X,"DELTA V=" ,F6.2," MV"
200 WRITE (15,150)YC(2),ZC(2)
210 DISP "CURRENT 3: I,DELTA V,B0,DELTA B=";
220 INPUT IC(3),WC(3),YC(3),ZC(3)
230 WRITE (15,240)IC(3),WC(3)
240 FORMAT "CURRENT 3: I=" ,F8.5," MA",2X,"DELTA V=" ,F6.2," MV"
250 WRITE (15,150)YC(3),ZC(3)
260 DISP "CURRENT 4: I,DELTA V,B0,DELTA B=";
270 INPUT IC(4),WC(4),YC(4),ZC(4)
280 WRITE (15,290)IC(4),WC(4)
290 FORMAT "CURRENT 4: I=" ,F8.5," MA",2X,"DELTA V=" ,F6.2," MV"
300 WRITE (15,150)YC(4),ZC(4)
310 A1=SQRT(1-(1.1811E+04/(F1+A*2))^2)/(375.73*B*2)
320 FOR N=1 TO 4
330 ZCNJ=ZCNJ-1
340 YCNJ=YCNJ
350 GCNJ=ICNJ*2.3026/(GCNJ*A1)
360 NEXT N
370 DISP "INTL VALUE:MSKR,IND.,POST CAP.=";
380 INPUT L,C1
390 WRITE (15,400)L,C1
400 FORMAT "INITIAL VALUES:MSKR,INDUCTANCE=" ,F6.3," NH POST CAP.=" ,F6.2,"
410 DISP "INTL VALUES: RES., TURNS RATIO=";
420 INPUT R,K
430 WRITE (15,440)R,K
440 FORMAT 14X,"RESISTANCE=" ,F6.2," OHM",3X,"INDUCTANCE=" ,F7.3
450 M=3*PI*F1
460 B1=C1*M*1E-06
470 L1=M*L
480 VC11=R/((R+L1+I2)*A1)
490 VC21=L1/((R+L1+I2)*A1)
500 VC31=B1/A1-VC12
510 VC41=K*12

```

```

520 FOR N=1 TO 4
530 FCN1=VC11-VC41*ZCNJ*(GCNJ*ZCNJ*VC41-VC21+2-VC11*(GCNJ-VC41*ZCNJ))
540 FCN2=FCN1-2*VC21*(VC31-VC41*YCNJ)-(VC11+GCNJ)*(VC31-VC41*YCNJ)*I2
550 NEXT N
560 PRINT SQRT(FC11+I2+FC21+FC31+I2+FC41+I2)
570 IF SQRT(FC11+I2+FC21+FC31+I2+FC41+I2)<1E-08 THEN 700
580 FOR N=1 TO 4
590 JCN,11=(VC41*ZCNJ-GCNJ)*(2*VC11-VC41*ZCNJ)+GCNJ*ZCNJ*VC41-VC21+I2
600 JCN,12=-2*(VC21*(VC31-VC41*YCNJ)-(VC31-VC41*YCNJ)*I2)
610 JCN,21=-2*(VC21*(VC11-VC41*ZCNJ)+VC11*(VC31-VC41*YCNJ)*I2)
620 JCN,31=-2*(VC21*(VC11+VC31-VC41*YCNJ)*(VC11+GCNJ))
630 JCN,41=ZCNJ*(VC11+I2+VC21+I2-2*(VC41*ZCNJ*GCNJ+VC41*ZCNJ*VC11-VC11*GCNJ))
640 JCN,42=ZCNJ*(VC21+I2+VC11*(VC31-VC41*YCNJ))*(VC11+GCNJ)
650 NEXT N
660 MAT J=INV(J)
670 MAT I=J*F
680 MAT V=Y*I
690 GOTO 520
700 R=VC11/((VC11+I2+VC21+I2)*A1)
710 L1=VC21/R/VC11
720 L=L1/M
730 C1=(VC31+VC21)*A1/(M*1E-06)
740 K=SQRT(VC41)
750 FOR N=1 TO 4
760 GCNJ=2*VC21*(VC11-VC41*ZCNJ)-(VC11+I2-VC21+I2)*(VC31-VC41*YCNJ)
770 FCN1=GCNJ/((VC11-VC41*ZCNJ)+I2*(VC31-VC41*YCNJ)+I2)*A1/(M*1E-06)
780 NEXT N
790 WRITE (15,800)R,L
800 FORMAT "FIRAL VALUES: RESISTANCE=" ,F6.2," OHM",3X,"INDUCTANCE=" ,F7.3
810 WRITE (15,820)C1,K
820 FORMAT 14X,"POST CAPACITANCE=" ,F6.2," FF TURNS RATIO=" ,F5.2
830 WRITE (15,840)
840 FORMAT "DIODE CAPACITANCES:"
850 FOR N=1 TO 4
860 WRITE (15,870)GCNJ,ICNJ
870 FORMAT 20X,"C=" ,F6.2," FF FOR I=" ,F8.5," MA"
880 NEXT N
890 GOTO 370
900 END

```

Program in File 1

Perfect match of the signal source to the waveguide has been assumed in the previous program. As explained in Section IV of the paper, this assumption can be relaxed if the data for five diode biases are used. But if one of the bias currents is large enough, so the diode differential conductance is much larger than the susceptance of the diode capacitance, the large current approximation, discussed in Section V of the paper, can be used. The large-current approximation of Equation (15) is

$$\Delta B^{(4)} - jB_o^{(4)} = y_{11} - \frac{(y_{12})^2}{g_d^{(4)}} \quad (A.16)$$

Superscript (4) has been used to denote large current data. This equation can be split into two independent equations:

$$\Delta B^{(4)} = g_{11} + \frac{b_{12}^2 - g_{12}^2}{g_d^{(4)}} \quad (A.17)$$

and

$$-B_o^{(4)} = b_{11} - \frac{2b_{12}g_{12}}{g_d^{(4)}} \quad (A.18)$$

It is now clear that only three equations of the form (A.10) have to be added to (A.17) and (A.18) to form the set of equations from which five elements (n , L_s , C_p , R_s , G_g) of the equivalent circuit can be found. This is done in the program to be described.

Equations (A.17) and (A.18), with the help of Equations (A.2) can be rewritten as

$$\Delta B^{(4)} = G_g + \frac{1}{n^2} \left(g + \frac{(b'_{12})^2 - g^2}{g_d^{(4)}} \right) \quad (A.19)$$

and

$$-B_o^{(4)} \approx b_{11}' = \frac{1}{n^2} \left(\omega C_p' - b_{12}' \right) = \frac{1}{n^2} b_{11}' \quad (A.20)$$

where g , b_{11}' , and b_{12}' are given by Equations (A.13). The finite $g_d^{(4)}$ has a much smaller effect on the input susceptance than on the input conductance; this effect has been entirely neglected in Equation (A.20). It should also be noted that the post capacitance C_p' now also contains the imaginary part of the admittance presented by the source. Now G_g is found from Equation (A.19) and substituted in Equation (A.12) to get

$$\left(g^2 - (b_{12}')^2 \right) \left[\frac{g^2 - (b_{12}')^2}{g_d^{(4)}} - (\Delta B^{(k)} - \Delta B^{(4)})n^2 \right] - 2b_{12}'g(b_{11}' + n^2 B_o^{(k)})$$

$$- (g + g_d^{(k)}) \left[\left[\frac{g^2 - (b_{12}')^2}{g_d^{(4)}} - (\Delta B^{(k)} - \Delta B^{(4)})n^2 \right]^2 + \left(b_{11}' + n^2 B_o^{(k)} \right)^2 \right] = 0 \quad (A.21)$$

Three equations of the form (A.21) and Equation (A.20) are then solved for n , g , b_{12}' , b_{11}' , i.e. for n , L_s , C_p , R_s . After this is done, diode capacitances $C_d^{(k)}$ ($k = 1, 2, 3$) are found from Equations (A.14) with G_g replacing Y_G .

The listing of the program and an example of the printout during execution are shown on the next pages. For reasons mentioned in the previous section, this program did not converge well for some sets of input data.

WAVEGUIDE DIMENSIONS IN MILLS A= 51.0 B= 6.4
 FREQUENCY= 152.80GHZ
 CURRENT 1: I= 0.00500 MA DELTA V= 67.90 MV
 B0/Y10= -2.925 DELTA B/Y10= 1.647
 CURRENT 2: I= 0.05000 MA DELTA V= 69.40 MV
 B0/Y10= -2.355 DELTA B/Y10= 2.719
 CURRENT 3: I= 0.50000 MA DELTA V= 70.50 MV
 B0/Y10= 0.126 DELTA B/Y10= 2.133
 HIGH CURRENT 4: I= 5.00000 MA DELTA V= 70.50 MV
 B0/Y10= 0.458 DELTA B/Y10= 1.467
 INITIAL VALUES: WSKR. INDUCTANCE= 0.110 NH POST CAP.= 6.20 F
 RESISTANCE= 25.00 OHM TURNS RATIO= 0.90
 0.110026638
 0.015067507
 1.30896E-03
 6.82033E-06
 1.53623E-11
 FINAL VALUES: RESISTANCE= 29.78 OHM INDUCTANCE= 0.108 NH
 POST CAPACITANCE= 6.66 FF TURNS RATIO= 0.89
 SOURCE VSWR= 1.09
 DIODE CAPACITANCES:
 C= 5.44 FF FOR I= 0.00500 MA
 C= 6.48 FF FOR I= 0.05000 MA
 C= 12.11 FF FOR I= 0.50000 MA

```

10 DIM FC[4],JC[4],VE[4],DE[4],Z[5],G[5],MC[5],IC[5],CE[4],XE[4],UC[4],EE[4]
20 DISP "WAVEGUIDE DIMENSIONS IN MILLS RB";
30 INPUT RB
40 WRITE (15,90)R,B
50 DISP "FREQUENCY =";
60 INPUT F1
70 WRITE (15,80)F1
80 FORMAT "FREQUENCY=",F7.2,"GHZ"
90 FORMAT "WAVEGUIDE DIMENSIONS IN MILLS",5X,"A=";F6.1,4X,"B=";F5.1
100 DISP "CURRENT 1:I,DELTA V;B0,DELTA B=";
110 INPUT IC1,MC1,YC1,ZC1
120 WRITE (15,130)IC1,MC1
130 FORMAT "CURRENT 1: I=";F8.5," MA",2X," DELTA V=";F6.2," MV"
140 WRITE (15,150)YC1,ZC1
150 FORMAT 10X,"B0/Y10=";F8.3,2X," DELTA B/Y10=";F8.3
160 DISP "CURRENT 2: I,DELTA V;B0,DELTA B=";
170 INPUT IC2,MC2,YC2,ZC2
180 WRITE (15,190)IC2,MC2
190 FORMAT "CURRENT 2: I=";F8.5," MA",2X," DELTA V=";F6.2," MV"
200 WRITE (15,150)YC2,ZC2
210 DISP "CURRENT 3: I,DELTA V;B0,DELTA B=";
220 INPUT IC3,MC3,YC3,ZC3
230 WRITE (15,240)IC3,MC3
240 FORMAT "CURRENT 3: I=";F8.5," MA",2X," DELTA V=";F6.2," MV"
250 DISP "HIGH CURRENT 4: I,DELTA V;B0,DELTA B=";
260 INPUT IC4,MC4,YC4,ZC4
270 WRITE (15,290)IC4,MC4
280 FORMAT "HIGH CURRENT 4: I=";F8.5," MA",2X," DELTA V=";F6.2," MV"
290 WRITE (15,150)YC4,ZC4
300 AI=A*SQR(1-(1.1811E+04/(F1*A*2))2)/(376.73*B*2)
310 FOR N=1 TO 3
320 Z[N]=Z[N]-Z[4]
330 Z[N]=Z[N]-Z[4]
340 NEXT N
350 FOR N=1 TO 4
360 YCNJ=-YCNJ
370 GCNJ=ICNJ*2.3026/(WCNJ*A1)
380 NEXT N
390 DISP "INTL VALUE:WSKR,IND.,POST CAP.=";
400 INPUT L,C1
410 WRITE (15,420)L,C1
420 FORMAT "INITIAL VALUES:WSKR,INDUCTANCE=";F6.3," NH POST CAP.=";F6.2," F
430 DISP "INTL VALUES: RES., TURNS RATIO=";
440 INPUT R,K
450 WRITE (15,460)R,K
460 FORMAT 14X,"RESISTANCE=";F6.2," OHM",3X," TURNS RATIO=";F5.2
470 M=2*PI*F1
480 BI=C1*M*1E-06
490 LI=M*L
500 VE1]=R/((R2+L12)*A1)
510 VE2]=LI/((R2+L12)*A1)
520 VE3]=BI/A1-VE2]
530 VE4]=K*2
540 FOR N=1 TO 3
550 XCNJ]=(VE1]2-VE2]2/GC4]-VE4]*Z[N]
560 UCNJ]=VE3]-VE4]*YCNJ
570 FINJ]=(VE1]2-VE2]2*XCNJ)-(VE1]+GCNJ]*XCNJ2-2*VE1]*VE2]*UCNJ
580 FLNJ]=FINJ-(VE1]+GCNJ)*UCNJ2
590 NEXT N
600 FC4]=VE3]-VE4]*YCNJ
610 PRINT SQR(FLNJ2+FLC2]2+FC3]2+FC4]2)<1E-08 THEN 800
620 IF SQR(FLNJ2+FLC2]2+FC3]2+FC4]2)<1E-08 THEN 800
630 FOR N=1 TO 3
640 JCN1]=2*VE1]*((VE1]2-VE2]2)/GC4]+XCNJ]-2*(VE1]+GCNJ)*XCNJ/GC4]
650 JCN1]=JCN1]-XCNJ2-UCNJ2-2*VE2]*UCNJ
660 JCN2]=2*VE2]*(2*(VE1]+GCNJ)*XCNJ/GC4]-XCNJ)-(VE1]2-VE2]2)/GC4]
670 JCN2]=JCN2]-2*VE1]*UCNJ
680 JCN3]=2*(VE2]*VE1]+UCNJ*(VE1]+GCNJ))
690 JCN4]=Z[N]*((VE1]2-VE2]2+2*(VE1]+GCNJ))*XCNJ+YCNJ*UCNJ)
700 JCN4]=JCN4]2+2*YCNJ*VE2]*VE1]
710 NEXT N
720 JC4,1]=0
730 JC4,2]=0
740 JC4,3]=1
750 JC4,4]=YCNJ
760 MAT J=INV(J)
770 MAT D=J*F
780 MAT V=V-D
790 GOTO 540
800 R=VE1]/(A1*(VE1]2+VE2]2))
810 LI=VE2]*R/VE1]
820 L=L1/M
830 C1=(VE3]+VE2])*A1/(M*1E-06)
840 K=SQR(VE4])
850 H=Z[4]-VE1]-VE2]2/GC4])/VE4]
860 FOR N=1 TO 3
870 ECNJ]=ZCNJ+Z[4]-H
880 C[NJ]=2*VE2]*VE1]*((VE1]-VE4]*ECNJ)-(VE1]2-VE2]2)*(VE3]-VE4]*YCNJ)
890 C[NJ]=(CCNJ)/((VE1]-VE4]*ECNJ)2+((VE3]-VE4]*YCNJ)2+VE2])*A1/(M*1E-06)
900 NEXT N
910 IF H>1 THEN 930
920 H=1/H
930 WRITE (15,940)R,L
940 FORMAT "FINAL VALUES: RESISTANCE=";F6.2," OHM",3X," INDUCTANCE=";F7.3," NH
950 WRITE (15,960)C1,K
960 FORMAT 14X,"POST CAPACITANCE=";F6.2," FF TURNS RATIO=";F5.2
970 WRITE (15,980)H
980 FORMAT 14X,"SOURCE VSWR=";F6.2
990 WRITE (15,1000)
1000 FORMAT "DIODE CAPACITANCES: "
1010 FOR N=1 TO 3
1020 WRITE (15,1030)C[NJ,ILN]
1030 FORMAT 20X,"C=";F6.2," FF FOR I=";F8.5," MA"
1040 NEXT N
1050 GOTO 390
1060 END

```

Program in File 2

This program is a simplification of the program in File 0. Both perfect match of the signal source, i.e. $Y_G = G = Y_g$, and the high-current approximation are assumed. This program therefore solves a set of four equations: two equations of the form given by (A.12), Equations (A.19) and (A.20).

The listing of the program and an example of the printout during execution are shown on the next pages. No case of poor convergence of this program for the experimental data for mixers A and B has been observed

```
WAVEGUIDE DIMENSIONS IN MILLS      A= 51.0      B= 6.4
FREQUENCY= 152.80GHZ
CURRENT 1: I= 0.00500 MA  DELTA V= 67.90 MV
          B0/Y10= -2.925  DELTA B/Y10=  1.647
CURRENT 2: I= 0.05000 MA  DELTA V= 69.40 MV
          B0/Y10= -2.355  DELTA B/Y10=  2.719
HIGH CURRENT 3: I= 5.00000 MA  DELTA V= 70.50 MV
          B0/Y10=  0.458  DELTA B/Y10=  1.467
INITIAL VALUES: WSKR. INDUCTANCE= 0.110 NH  POST CAP.= 6.60 FF
                  RESISTANCE= 25.00 OHM  TURNS RATIO= 0.90
0.091653969
0.015826193
7.01888E-04
1.84917E-05
1.50965E-06
1.17852E-07
9.20301E-09
FINAL VALUES: RESISTANCE= 26.10 OHM  INDUCTANCE= 0.112 NH
                POST CAPACITANCE= 6.50 FF  TURNS RATIO= 0.89
DIODE CAPACITANCES:
                C= 5.24 FF  FOR I= 0.00500 MA
                C= 6.10 FF  FOR I= 0.05000 MA
```

```

10 DIM F[4],J[4],I[4],Z[4],DE[4],VE[4],GE[4],ME[4],IL[4],CL[4]
20 DISP "WAVEGUIDE DIMENSIONS IN MILLS R,B;"
30 INPUT R,B
40 WRITE (15,90)R,B
50 DISP "FREQUENCY =";
60 INPUT F1
70 WRITE (15,80)F1
80 FORMAT "FREQUENCY=",F7.2,"GHZ"
90 FORMAT "WAVEGUIDE DIMENSIONS IN MILLS",5X,"R=",F6.1,4X,"B=",F5.1
100 DISP "CURRENT 1, DELTA V, B0, DELTA B=";
110 INPUT I[1],ME[1],YE[1],Z[1]
120 WRITE (15,130)I[1],ME[1]
130 FORMAT "CURRENT 1: I=",F8.5," MA",2X,"DELTA V=",F6.2," MV"
140 WRITE (15,150)Y[1],Z[1]
150 FORMAT 10X,"B0/Y10=",F8.3,2X,"DELTA B/Y10=",F8.3
160 DISP "CURRENT 2: I, DELTA V, B0, DELTA B=";
170 INPUT I[2],ME[2],YE[2],Z[2]
180 WRITE (15,190)I[2],ME[2]
190 FORMAT "CURRENT 2: I=",F8.5," MA",2X,"DELTA V=",F6.2," MV"
200 WRITE (15,150)Y[2],Z[2]
210 DISP "HIGH CURRENT 3: I, DELTA V, B0, DELTA B=";
220 INPUT I[3],ME[3],YE[3],Z[3]
230 WRITE (15,240)I[3],ME[3]
240 FORMAT "HIGH CURRENT 3: I=",F8.5," MA",2X,"DELTA V=",F6.2," MV"
250 WRITE (15,150)Y[3],Z[3]
260 A1=RSQR(1-(1.1811E+04/(F1*R*2)))^2)/(376.73*R*2)
270 FOR N=1 TO 3
280 Z[N]=Z[N]-1
290 Y[N]=Y[N]
300 G[N]=I[N]*2.3026/(ME[N]*R1)
310 NEXT N
320 DISP "INTL. VALUE: MSKR. IND., POST CAP. =";
330 INPUT L,C1
340 WRITE (15,350)L,C1
350 FORMAT "INITIAL VALUES: MSKR. INDUCTANCE=",F6.3," NH POST CAP.=",F6.2," FF"
360 DISP "INTL. VALUES: RES., TURNS RATIO=";
370 INPUT R,K
380 WRITE (15,390)R,K
390 FORMAT 14X,"RESISTANCE=",F6.2," OHM",3X,"TURNS RATIO=",F5.2
400 M=2*PI*F1
410 B1=C1*M*1E-06
420 L1=M*L
430 V1=I[R]/(R1*(R^2+L1^2))
440 V2=L1/(R1*(R^2+L1^2))
450 V3=B1/R1-V2
460 V4=K^2
470 FOR N=1 TO 2
480 FCN1=(V1-V4)*Z[N]**(G[N]*Z[N]*VE[4]-VE[2]*2)-(V1-V4)*Z[N]**(G[N]-VE[4]*Z[N])
490 FCN2=(V1-V4)*Z[N]**(G[N]*Z[N]*VE[4]-VE[2]*2)-(V1-V4)*Z[N]**(G[N]-VE[4]*Z[N])
500 NEXT N
510 FC3=V1-V2-VE[3]*Z[3]
520 FL4=VE[3]-VE[4]*Z[3]
530 PRINT SQR(FL1)^2+FL2^2+FL3)^2+FL4)^2)
540 IF SQR(FL1)^2+FL2)^2+FL3)^2+FL4)^2)<1E-08 THEN 750
550 FOR N=1 TO 2
560 J[N,1]=(V[4]*Z[N]-G[N])*(2*V[1]-V[4]*Z[N])+G[N]*Z[N]*VE[4]-VE[2]*2
570 J[N,2]=J[N,1]-2*V[2]*(V[3]-V[4]*Z[N])-(V[3]-VE[4]*Z[N])^2
580 J[N,3]=2*(V[2]*(V[1]-V[4]*Z[N])+V[1]*(V[3]-VE[4]*Z[N]))
590 J[N,4]=2*(V[2]*V[1]+(V[3]-VE[4]*Z[N])*(V[1]+G[N]))
600 J[N,5]=Z[N]*(V[1]^2+VE[2]^2-2*(V[4]*Z[N]*G[N]+VE[4]*Z[N]*VE[1]-V[1]*G[N]))
610 J[N,6]=J[N,4]+2*(V[2]*V[1]+(V[3]-VE[4]*Z[N])*(V[1]+G[N]))
620 NEXT N
630 J[3,1]=2*V[1]-G[3]
640 J[3,2]=2*V[2]
650 J[3,3]=0
660 J[3,4]=G[3]*Z[3]
670 J[4,1]=0
680 J[4,2]=0
690 J[4,3]=1
700 J[4,4]=Y[3]
710 MAT J=INV(J)
720 MAT D=J*F
730 MAT V=D
740 GOTO 470
750 R=V[1]/(R1*(V[1]-VE[4]*Z[N])-(V[1]^2-VE[2]*2))*(V[3]-VE[4]*Z[N])
760 L1=V[2]*R/V[1]
770 L=L1/M
780 C1=(V[3]+V[2])*R1/(M*1E-06)
790 K=SQR(V[4])
800 FOR N=1 TO 2
810 C[N]=-2*V[2]*V[1]*(V[1]-VE[4]*Z[N])-(V[1]^2-VE[2]*2)*(V[3]-VE[4]*Z[N])
820 CLN=(CLN)/((V[1]-VE[4]*Z[N])^2+(V[3]-VE[4]*Z[N])^2)+V[2])*(V[3]-VE[4]*Z[N])
830 NEXT N
840 WRITE (15,850)R,L
850 FORMAT "FINAL VALUES: RESISTANCE=",F6.2," OHM",3X,"INDUCTANCE=",F7.3," NH
860 WRITE (15,870)C1,K
870 FORMAT 14X,"POST CAPACITANCE=",F6.2," FF TURNS RATIO=",F5.2
880 WRITE (15,890)
890 FORMAT "DIODE CAPACITANCES:"
900 FOR N=1 TO 2
910 WRITE (15,920)C[N],I[N]
920 FORMAT 20X,"C=",F6.2," FF FOR I=",F8.5," MA"
930 NEXT N
940 GOTO 320
950 END

```

Program in File 3

This program employs further simplification of the problem. Not only is the signal source assumed to be perfectly matched, but also the diode capacitance for each bias is assumed to be known. Thus, the complex diode admittance $g_d^{(k)} + j\omega C_d^{(k)}$ is assumed to be known for every diode bias. As the embedding network consists now of four unknown elements, C_p , L_s , R_s , n , only two measurements are needed to determine them.

The program solves the two complex equations of the form

$$\Delta B^{(k)} - jB_o^{(k)} = Y_g + \frac{1}{n^2} \left\{ \frac{R_d^{(k)} + R_s}{(X_d^{(k)} + X_s)^2 + (R_d^{(k)} + R_s)^2} + j \left[B_p - \frac{X_d^{(k)} + X_s}{(X_d^{(k)} + X_s)^2 + (R_d^{(k)} + R_s)^2} \right] \right\} \quad (\text{A.22})$$

where

$$X_s = \omega L_s, \quad B_p = \omega C_p, \quad R_d = \frac{g_d^{(k)}}{(g_d^{(k)})^2 + (\omega C_d^{(k)})^2},$$
$$X_d = - \frac{\omega C_d^{(k)}}{(g_d^{(k)})^2 + (\omega C_d^{(k)})^2} \quad (\text{A.23})$$

The program listing and an example of the printout during execution are shown on the following pages.

No case of poor convergence of this program for the experimental data for mixers A and B has been observed.

WAVEGUIDE DIMENSIONS IN MILLS A= 51.0 B= 6.4
FREQUENCY= 152.80GHZ
LOW CURRENT 1: I= 0.00500 MA DELTA V= 67.90 MV
 B0/G10= -2.925 DELTA B/G10= 1.647
 CAPACITANCE= 5.24 FF
LOW CURRENT 2: I= 0.05000 MA DELTA V= 69.40 MV
 B0/G10= -2.355 DELTA B/G10= 2.719
 CAPACITANCE= 6.10 FF
INITIAL VALUES: WSKR. INDUCTANCE= 0.110 NH POST CAP.= 6.60
 RESISTANCE= 25.00 OHM TURNS RATIO= 0.90
0.057267202
3.87774E-04
2.19098E-06
8.24621E-12
FINAL VALUES: RESISTANCE= 26.16 OHM INDUCTANCE= 0.113 NH
 POST CAPACITANCE= 6.52 FF TURNS RATIO= 0.89

```

10 DIM FL(4),JC(4),VC(4),DC(4)
20 DISP "WAVEGUIDE DIMENSIONS IN MILLS A,B";
30 INPUT A,B
40 WRITE (15,90)A,B
50 DISP "FREQUENCY =";
60 INPUT F1
70 WRITE (15,80)F1
80 FORMAT "FREQUENCY=",F7.2,"GHZ"
90 FORMAT "WAVEGUIDE DIMENSIONS IN MILLS",5X,"A=",F6.1,4X,"B=",F5.1
100 DISP "CURRENT 1: I,DELTA V,B0,DELTA B,CAP.=";
110 INPUT I1,V1,Y1,Z1,C1
120 WRITE (15,130)I1,V1
130 FORMAT "LOW CURRENT 1: I=",F8.5," MA ",2X,"DELTA V=",F6.2," MV"
140 WRITE (15,150)Y1,Z1
150 FORMAT "I1X",B0,G10=","F7.3,2X,"DELTA B/G10=","F7.3
160 WRITE (15,170)C1
170 FORMAT "I1X","CAPACITANCE=",F6.2," FF"
180 DISP "CURRENT 2: I,DELTA V,B0,DELTA B=CAP.=";
190 INPUT I2,V2,Y2,Z2,C2
200 WRITE (15,210)I2,V2
210 FORMAT "LOW CURRENT 2: I=",F8.5," MA ",2X,"DELTA V=",F6.2," MV"
220 WRITE (15,240)C2
240 FORMAT "I2X","CAPACITANCE=",F6.2," FF"
250 A1=A*SQR(1-(1.1811E+04/(F1*A*2))2)/(376.73*B*2)
260 G1=I1*2.3026/(V1*A1)
270 G2=I2*2.3026/(V2*A1)
280 M=2*PI*F1
290 B1=C1*M*1E-06/A1
300 B2=C2*M*1E-06/A1
310 M1=G12+B12
320 R1=G1/M1
330 X1=-B1/M1
340 M2=G22+B22
350 R2=G2/M2
360 X2=-B2/M2
370 Z1=Z1-1
380 Z2=Z2-1
390 DISP "INTL.VALUES:MSKR,IND.,POST.CAP.=";
400 INPUT L,C
410 WRITE (15,420)L,C
420 FORMAT "INITIAL VALUES:MSKR,INDUCTANCE=",F6.3," NH POST CAP.=",F6.2," F1"
430 DISP "INTL.VALUES:RES.,TURNS RATIO=";
440 INPUT R,N
450 WRITE (15,460)R,N
460 FORMAT "R1X","RESISTANCE=",F6.2," OHM",3X,"TURNS RATIO=",F5.2
470 V1=V1*M*L*A1
480 V2=V2*A1
490 V13=C*M*1E-06/A1
500 V14=1/N
510 F11=X1+V11-(V14)2*V13+Y1*(R1+V12))/Z1
520 F12=X2+V11-(V14)2*V13+Y2*(R2+V12))/Z2
530 F13=V142*(R1+V12)-Z1*(X1+V11)2+(R1+V12)2
540 F14=V142*(R2+V12)-Z2*(X2+V11)2+(R2+V12)2
550 PRINT SQR(F11)2+F122+F132+F142
560 IF SQR(F11)2+F122+F132+F142<1E-08 THEN 770
570 JC(1,1)=1
580 JC(1,2)=-V142*V13+Y1)/Z1
590 JC(1,3)=-V142*V13+Y2)/Z2
600 JC(1,4)=-2*V142*V13*(R1+V12))/Z1
610 JC(2,1)=1
620 JC(2,2)=-V142*V13+Y2)/Z2
630 JC(2,3)=-V142*V13+Y2)/Z2
640 JC(2,4)=-2*V142*V13*(R2+V12))/Z2
650 JC(3,1)=-2*Z1*(X1+V11)
660 JC(3,2)=V142-2*Z1*(R1+V12)
670 JC(3,3)=0
680 JC(3,4)=2*V142*(R1+V12)
690 JC(4,1)=-2*Z2*(X2+V11)
700 JC(4,2)=V142-2*Z2*(R2+V12)
710 JC(4,3)=0
720 JC(4,4)=2*V142*(R2+V12)
730 MAT J=INV(J)
740 MAT V=V-D
750 MAT V=V-D
760 GOTO 510
770 L=V11/(M*A1)
780 R=V12/A1
790 C=V13*A1/(M*1E-06)
800 N=1/V14
810 WRITE (15,820)R,L
820 FORMAT "FINAL VALUES: RESISTANCE=",F6.2," OHM",3X,"INDUCTANCE=",F7.3," NH"
830 WRITE (15,840)C,N
840 FORMAT "POST CAPACITANCE=",F6.2," FF TURNS RATIO=",F5.2
850 GOTO 390
860 END

```

Program in File 4

This is a simpler version of the program in File 2. The signal source is assumed to be perfectly matched, the transformer turns ratio is assumed to be known, and the high-current approximation is also used.

The program therefore solves a set of three equations to find R_s , L_s , and C_p . Two of the equations have the form given by Equation (A.12); the third is Equation (A.20). The diode capacitances $C_d^{(k)}$ for the two smaller currents are then found from an equation of the form given by (A.14).

The program listing and an example of the printout during execution follows.

No case of poor convergence of this program for the experimental data for mixers A and B has been observed. This is the program that was used in the computational procedure described in Section V of the paper.

```
WAVEGUIDE DIMENSIONS IN MILLS      A= 51.0      B= 6.4
FREQUENCY= 152.80GHZ
TRANSFORMER TURNS RATIO= 0.90
CURRENT 1: I= 0.00500 MA  DELTA V= 67.90 MV
          B0/Y10= -2.925  DELTA B/Y10=  1.647
CURRENT 2: I= 0.05000 MA  DELTA V= 69.40 MV
          B0/Y10= -2.355  DELTA B/Y10=  2.719
HIGH CURRENT 3: I= 5.00000 MA  B0=  0.458
INITIAL VALUES: WSKR. INDUCTANCE= 0.110 NH  POST CAP.=  6.20 FF
                   RESISTANCE= 25.00 OHM
0.095193012
2.34324E-03
2.37986E-07
3.60555E-11
FINAL VALUES: RESISTANCE= 25.21 OHM  INDUCTANCE=  0.111 NH
                POST CAPACITANCE=  6.56 FF
DIODE CAPACITANCES:
          C=  5.33 FF  FOR I= 0.00500 MA
          C=  6.18 FF  FOR I= 0.05000 MA
```

```

10 DIM FC3,J3,I3,Z3,VC3,ZC3,IC3,MC3,VC3,IC3,IC2J
20 DISP "WAVEGUIDE DIMENSIONS IN MILLS R,B";
30 INPUT R,B
40 WRITE (15,130)R,B
50 DISP "FREQUENCY =";
60 INPUT F1
70 WRITE (15,80)F1
80 FORMAT "FREQUENCY=",F7.2,"GHZ"
90 DISP "TRANSFORMER TURNS RATIO=";
100 INPUT K1
110 WRITE (15,120)K1
120 FORMAT "TRANSFORMER TURNS RATIO=",F5.2
130 FORMAT "WAVEGUIDE DIMENSIONS IN MILLS",5X,"A=",F6.1,4X,"B=",F5.1
140 DISP "CURRENT 1: I, DELTA V, B0, DELTA B=";
150 INPUT IC1J,MC1J,VC1J,ZC1J
160 WRITE (15,170)IC1J,MC1J
170 FORMAT "CURRENT 1: I=",F8.5," MA",2X,"DELTA V=",F6.2," MV"
180 WRITE (15,190)VC1J,ZC1J
190 FORMAT 10X,"B0/Y10=",F8.3,2X,"DELTA B/Y10=",F8.3
200 DISP "CURRENT 2: I, DELTA V, B0, DELTA B=";
210 INPUT IC2J,MC2J,VC2J,ZC2J
220 WRITE (15,230)IC2J,MC2J
230 FORMAT "CURRENT 2: I=",F8.5," MA",2X,"DELTA V=",F6.2," MV"
240 WRITE (15,190)VC2J,ZC2J
250 DISP "HIGH CURRENT 3: I, B0=";
260 INPUT IC3J,VC3J
270 WRITE (15,280)IC3J,VC3J
280 FORMAT "HIGH CURRENT 3: I=",F8.5," MA",2X,"B0=",F8.3
290 A1=A*SR((1-(1.1811E+04/(F1**2))**2)/(376.73*B**2)
300 FOR N=1 TO 2
310 ZCNJ=ZCNJ-1
320 YCNJ=-YCNJ
330 GCNJ=ICNJ*2.3026/(MCNJ*A1)
340 NEXT N
350 DISP "INTL. VALUES: WSKR, IND., POST CAP. =";
360 INPUT L,C1
370 WRITE (15,380)L,C1
380 FORMAT "INITIAL VALUES: WSKR, INDUCTANCE=",F6.3," NH POST CAP.=",F6.2," FF"
390 DISP "INTL. VALUES: RESISTANCE=";
400 INPUT R
410 WRITE (15,420)R
420 FORMAT 14X,"RESISTANCE=",F6.2," OHM"
430 M=2*PI*F1
440 B1=C1*M*1E-06
450 L1=M*L
460 VC1J=R/(A1*(R**2+L1**2))
470 VC2J=L1/(A1*(R**2+L1**2))
480 VC3J=B1/A1-VC2J
490 K=K1**2
500 FOR N=1 TO 2
510 FCNJ=(VC1J-K*ZCNJ)*(GCNJ+ZCNJ-K-VC2J**2)-(VC1J-K*ZCNJ)**2
520 FCNJ=FCNJ-2*VC2J*VC1J+(VC3J-K*YCNJ)-(VC1J+GCNJ)*(VC3J-K*YCNJ)**2
530 NEXT N
540 FC3J=VC3J+K*YCNJ
550 PRINT SR(FC1J**2+FC2J**2+FC3J**2)<1E-08 THEN 700
560 IF SR(FC1J**2+FC2J**2+FC3J**2)<1E-08 THEN 700
570 FOR N=1 TO 2
580 JCN,1J=(K*ZCNJ-GCNJ)*(2*VC1J-K*ZCNJ)+GCNJ*ZCNJ-K-VC2J**2
590 JCN,1J=JCN,1J-2*VC2J*(VC3J-K*YCNJ)-(VC3J-K*YCNJ)**2
600 JCN,2J=-2*(VC2J*(VC1J-K*ZCNJ)+VC1J*(VC3J-K*YCNJ))
610 JCN,3J=-2*(VC2J*VC1J+(VC3J-K*YCNJ))*(VC1J+GCNJ)
620 NEXT N
630 JCN,1J=0
640 JCN,2J=0
650 JCN,3J=1
660 MAT J=INV(J)
670 MAT D=J*F
680 MAT V=V-D
690 GOTO 500
700 R=VC1J/(A1*(VC1J**2+VC2J**2))
710 L=L1/M
720 C1=(VC3J+VC2J)*A1/(M*1E-06)
730 C1=(VC3J+VC2J)*A1/(M*1E-06)
740 FOR N=1 TO 2
750 CCNJ=-2*VC2J*VC1J*(VC1J-K*ZCNJ)-(VC1J**2-VC2J**2)*(VC3J-K*YCNJ)
760 CCNJ=(CCNJ)/(VC1J-K*ZCNJ)**2+(VC3J-K*YCNJ)**2+VC2J**2)*A1/(M*1E-06)
770 NEXT N
780 WRITE (15,790)R,L
790 FORMAT "FINAL VALUES: RESISTANCE=",F6.2," OHM",3X,"INDUCTANCE=",F7.3," NH"
800 WRITE (15,810)C1
810 FORMAT 14X,"POST CAPACITANCE=",F6.2," FF"
820 WRITE (15,830)
830 FORMAT "DIODE CAPACITANCES:"
840 FOR N=1 TO 2
850 WRITE (15,860)CCNJ,ICNJ
860 FORMAT 20X,"C=",F6.2," FF FOR I=",F8.5," MA"
870 NEXT N
880 GOTO 350
890 END

```

A.2.2. Programs for Analyzing Mixer Mount Equivalent Circuits

The programs described in this section were used for analysis of the properties of the mounts once their equivalent circuits had been established.

Program in File 5

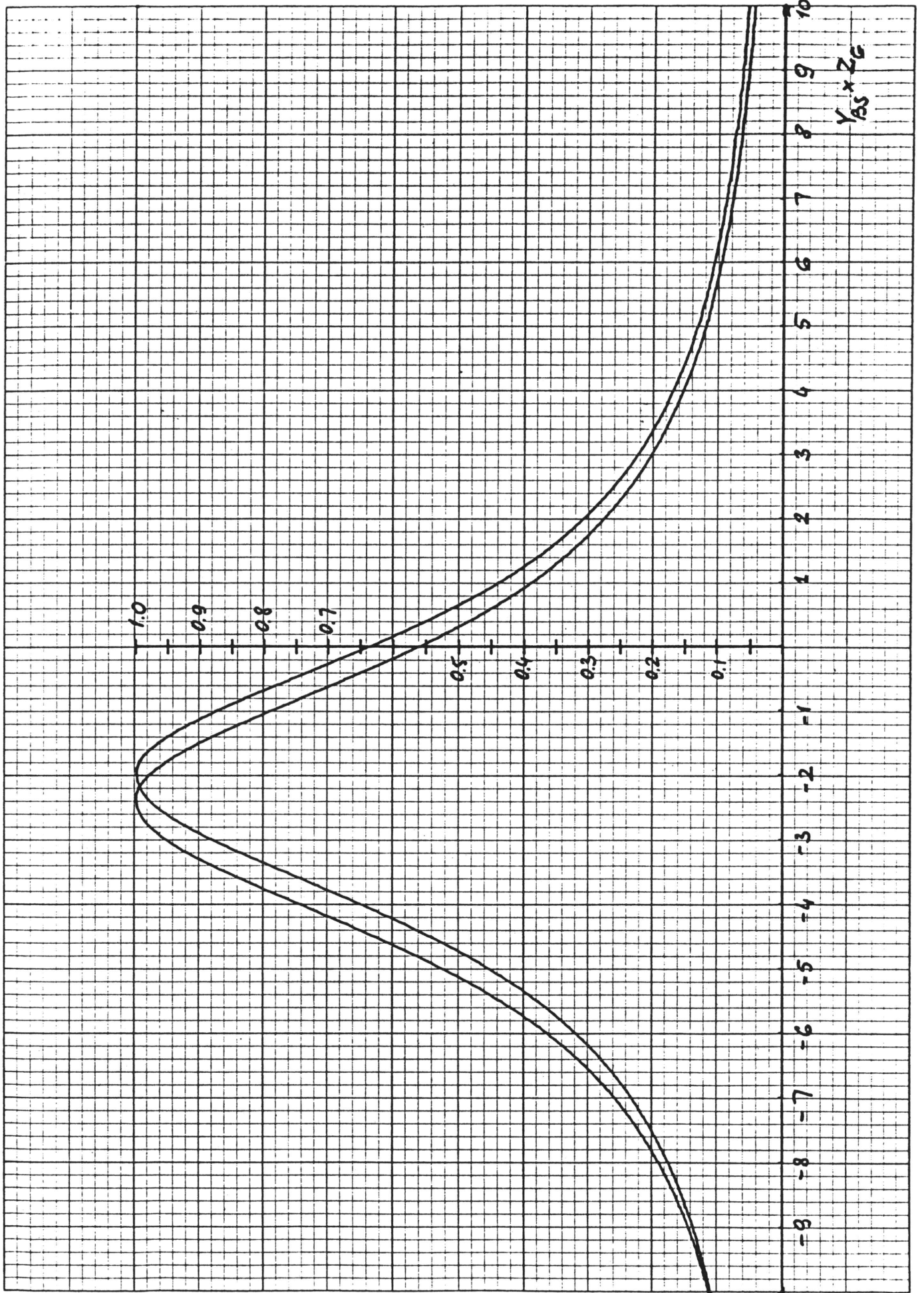
This program plots the $\Delta I = f(Y_{BS} \times Z_G)$ curve for a given equivalent circuit. It assumes that the signal source is perfectly matched to the waveguide. It can therefore be used for checking the agreement between the measured points and the curves computed from the equivalent circuit. The determination of the equivalent circuit is always based on the assumption that the backshort and its containing waveguide are lossless. This program, however, allows both of these losses to be taken into account. The user can specify the attenuation constant of the waveguide (in nepers/mil) and also the backshort series resistance. This resistance replaces the short circuit in the model and therefore can account for the losses in the backshort itself. The analysis can be performed for the backshort assuming positions within the range $\left\{ (k-1) \frac{\lambda g}{2}, k \frac{\lambda g}{2} \right\}$, where k is an integer specified by the user.

The minimum transducer attenuation is computed for every curve. This is defined as the ratio of power delivered to the diode incremental conductance to the available power of the generator, having internal conductance equal to the waveguide characteristic admittance. The minimum transducer attenuation corresponds to a peak of the $\Delta I = f(Y_{BS} \times Z_G)$ curve. For comparison, the minimum transducer attenuation for the loss-free case is also computed.

The program listing and an example of the printout and plot during execution are shown on the following pages.

WAVEGUIDE DIMENSIONS IN MILLS A= 51.0 B= 6.4
FREQUENCY= 152.80GHZ
POST CAPACITANCE= 6.63 FF WHISKER INDUCTANCE= 0.110 NH
TRANSFORMER TURNS RATIO= 0.90
CURRENT= 0.0500MA DELTA V= 69.40MV
CAPACITANCE= 6.23 FF RESISTANCE= 24.90 OHM
WAVEGUIDE ATT. CONSTANT= 1.000E-04 N/MIL
DIODE-BS.DISTANCE IN HALF-WAVELENGTH= 1
BACK SHORT SERIES RESISTANCE= 0.00 OHM
MINIMUM TRANSDUCER ATTENUATION(LOSS FREE CASE)= 2.295DB
MINIMUM TRANSDUCER ATTENUATION(LOSSY CASE)= 2.328DB

CURRENT= 0.0500MA DELTA V= 69.40MV
CAPACITANCE= 6.23 FF RESISTANCE= 24.90 OHM
WAVEGUIDE ATT. CONSTANT= 1.000E-04 N/MIL
DIODE-BS.DISTANCE IN HALF-WAVELENGTH= 1
BACK SHORT SERIES RESISTANCE= 5.00 OHM
MINIMUM TRANSDUCER ATTENUATION(LOSS FREE CASE)= 2.295DB
MINIMUM TRANSDUCER ATTENUATION(LOSSY CASE)= 2.938DB



```

10 DIM YC(201),PI(201)
20 SCALE =10,10,0,1
30 XAXIS 0,1
40 YAXIS 0,0,05
50 DEF FNS(W)=(EXP(W)-EXP(-W))/2
60 DEF FNC(W)=(EXP(W)+EXP(-W))/2
70 DISP "WAVEGUIDE DIMENSIONS IN MILLS A,B;"
80 INPUT A,B
90 WRITE (15,170)A,B
100 DISP "FREQUENCY =" ;
110 INPUT F
120 WRITE (15,140)F
130 FORMAT "CAPACITANCE=",F6.2," FF RESISTANCE=",F6.2," OHM"
140 FORMAT "FREQUENCY=",F7.2,"GHZ"
150 FORMAT "POST CAPACITANCE=",F6.2," FF WHISKER INDUCTANCE=",F6.3," NH"
160 FORMAT "CURRENT=",F7.4," MA DELTA V=",F6.2," MV"
170 FORMAT "WAVEGUIDE DIMENSIONS IN MILLS",5X,"A=",F6.1,4X,"B=",F5.1
180 DISP "POST CAP. MSKR.IND.=";
190 INPUT C2,L
200 WRITE (15,150)C2,L
210 DISP "TRANSFORMER TURNS RATIO=";
220 INPUT W
230 WRITE (15,240)W
240 FORMAT "TRANSFORMER TURNS RATIO=",F5.2
250 DISP "CURRENT,DELTA V=";
260 INPUT I,V
270 WRITE (15,160)I,V
280 DISP " DIODE CAP.,RESISTANCE=";
290 INPUT C,R
300 WRITE (15,130)C,R
310 DISP "WAVEGUIDE ATT. CONSTANT=";
320 INPUT S1
330 WRITE (15,340)S1
340 FORMAT "WAVEGUIDE ATT. CONSTANT=",E11.3," N/MIL"
350 DISP "DIODE-BS.DIST. IN HALF-WL.=";
360 INPUT K
370 WRITE (15,380)K
380 FORMAT "DIODE-BS.DISTANCE IN HALF-WAVELENGTH=",F3.0
390 DISP "BACK SHORT SERIES RESISTANCE";
400 INPUT S2
410 WRITE (15,420)S2
420 FORMAT "BACK SHORT SERIES RESISTANCE=",F6.2," OHM"
430 B1=2*PI*F*C*1E-06
440 X1=2*PI*F*L
450 B2=X1/(R1+X1+I2)
460 G5R/(R1+X1+I2)
470 B3=B1-B2
480 G1=1+2.3026/V
490 B4=(B3*(B2+2-G+I2)-2*G*B2*(G1+G))/ (B3+I2+(G+G1)+I2)
500 D1=50R*(1-(1.1811E+04/(F*A*2))+I2)
510 D2=2*PI*F*D1/1.1811E+04
520 Z=376.73*B*2/(A*D1*W*2)
530 S2=S2/W*2
540 G2=(1-S1/D2)/Z
550 R1=G1/2+G*(1/Z+G1)+B2+2-B4*B3
560 I1=B4*G1+B3/2+G*(B4+B3+2*B2)
570 P1=-10*LG(4*G1*(G2+2*B2+I1+I2))/ (Z*(R1+2+I1+I2))
580 WRITE (15,590)P1
590 FORMAT "MINIMUM TRANSDUCER ATTENUATION(LOSS FREE CASE)=",F8.3," DB"
600 B5=2*PI*F*C*1E-06
610 FOR I=1 TO 201
620 Y(I)=-10+(I-1)*0.1
630 Y1=2*(PI/2+ATN(Y(I)))+(K-1)*PI
640 Y2=Y1*S1/D2
650 D=FNC(Y2)-COS(Y1)
660 U=FNS(Y2)/D
670 V=-SIN(Y1)/D
680 G3=S1/D2*Z
690 U2=U+G2*S2
700 V2=V+G3*S2
710 U3=U2*G2-G3*V2
720 V3=U2*G3+G2*V2
730 U4=S2*(U*G2-V*G3)+1
740 V4=S2*(U*G3+V*G2)
750 M=U4+2+V4+2
760 U1=(U3*U4+V3*V4)/M
770 V1=(V3*U4-U3*V4)/M
780 B5=V1+B5-B2
790 R3=G1*(G2+U1)+G*(G2+U1+G1)-B3*B5+B2+2
800 I3=B6*G1+B3*(G2+U1)+G*(B6+B3+2*B2)
810 P(I)=R3+2+I3+2
820 NEXT I
830 FOR I=2 TO 200
840 IF P(I)<P(I+1) THEN 860
850 NEXT I
860 J=I
870 P2=-10*LG(4*G1*G2*(G2+2*B2+I2))/P(I)
880 WRITE (15,890)P2
890 FORMAT "MINIMUM TRANSDUCER ATTENUATION(LOSSY CASE)=",F8.3," DB"
900 FOR I=1 TO 201
910 PLOT Y(I),P(I),P(I)
920 NEXT I
930 PEN
940 GOTO 250
950 END

```


Program in File 6

The program in File 6 is the version of the program in File 5 for the case of a lossless backshort and associated waveguide. It is therefore much faster. The program listing and an example of the printout during execution are shown on the following pages. The plots generated by the program are of the same form as those for the program in File 5.

WAVEGUIDE DIMENSIONS IN MILLS A= 51.0 B= 6.
FREQUENCY= 152.80GHZ
POST CAPACITANCE= 6.63 FF WHISKER INDUCTANCE= 0.
TRANSFORMER TURNS RATIO= 0.90
CURRENT= 5.0000 MA DELTA V= 70.50 MV
CAPACITANCE= 30.00 FF RESISTANCE= 24.90 OHM
MINIMUM TRANSDUCER ATTENUATION= 7.778DB

CURRENT= 1.0000 MA DELTA V= 70.50 MV
CAPACITANCE= 14.45 FF RESISTANCE= 24.90 OHM
MINIMUM TRANSDUCER ATTENUATION= 2.984DB

CURRENT= 0.5000 MA DELTA V= 70.50 MV
CAPACITANCE= 10.18 FF RESISTANCE= 24.90 OHM
MINIMUM TRANSDUCER ATTENUATION= 1.926DB

CURRENT= 0.2000 MA DELTA V= 70.50 MV
CAPACITANCE= 8.02 FF RESISTANCE= 24.90 OHM
MINIMUM TRANSDUCER ATTENUATION= 1.799DB

CURRENT= 0.0500 MA DELTA V= 69.40 MV
CAPACITANCE= 6.23 FF RESISTANCE= 24.90 OHM
MINIMUM TRANSDUCER ATTENUATION= 2.295DB

CURRENT= 0.0200 MA DELTA V= 69.00 MV
CAPACITANCE= 5.87 FF RESISTANCE= 24.90 OHM
MINIMUM TRANSDUCER ATTENUATION= 3.458DB

CURRENT= 0.0050 MA DELTA V= 67.90 MV
CAPACITANCE= 5.34 FF RESISTANCE= 24.90 OHM
MINIMUM TRANSDUCER ATTENUATION= 7.105DB

```

10 SCALE -10,10,0,1
20 XAXIS 0,1
30 YAXIS 0,0.05
40 DIM M[201],P[201]
50 DISP "WAVEGUIDE DIMENSIONS IN MILLS A,B";
60 INPUT A,B
70 WRITE (15,210)A,B
80 DISP "FREQUENCY =";
90 INPUT F
100 WRITE (15,180)F
110 DISP "POST CAP., WSKR.IND.=";
120 INPUT C2,L
130 WRITE (15,190)C2,L
140 DISP "TRANSFORMER TURNS RATIO=";
150 INPUT K
160 WRITE (15,230)K
170 FORMAT "CAPACITANCE=",F6.2," FF RESISTANCE=",F6.2," OHM"
180 FORMAT "FREQUENCY=",F7.2," GHZ"
190 FORMAT "POST CAPACITANCE=",F6.2," FF WHISKER INDUCTANCE=",F6
200 FORMAT "CURRENT=",F7.4," MA DELTA V=",F6.2," MV"
210 FORMAT "WAVEGUIDE DIMENSIONS IN MILLS",5X,"A=",F5.1,4X,"B=",F5
220 DISP "CURRENT,DELTA V=";
230 FORMAT "TRANSFORMER TURNS RATIO=",F5.2
240 INPUT I,V
250 WRITE (15,200)I,V
260 DISP " DIODE CAP.,RESISTANCE=";
270 INPUT C,R
280 WRITE (15,170)C,R
290 B1=2*PI*F*C*1E-06
300 X1=2*PI*F*L
310 B2=X1/(R^2+X1^2)
320 G=R/(R^2+X1^2)
330 B3=B1-B2
340 G1=I*2.3026/V
350 B4=(B3*(B2^2-G^2)-2*G*B2*(G1+G))/(B3^2+(G+G1)^2)
360 Z1=376.73*B^2/(A*SQR(1-(1.1811E+04/(F*A^2))^2)*K^2)
370 R1=G1/Z1+G*(1/Z1+G1)+B2^2-B4*B3
380 I1=B4*G1+B3/Z1+G*(B4+B3+2*B2)
390 P1=-10*LGT(4*G1*(G^2+B2^2)/(Z1*(R1^2+I1^2)))
400 WRITE (15,410)P1
410 FORMAT "MINIMUM TRANSDUCER ATTENUATION=",F8.3," DB"
420 B5=2*PI*F*C2*1E-06
430 R2=G1/Z1+G*(1/Z1+G1)+B2^2
440 FOR I=1 TO 201
450 Y=-10+(I-1)*0.1
460 M[I]=-B2+Y/Z1+B5
470 R3=R2-M[I]*B3
480 I3=M[I]*G1+B3/Z1+G*(M[I]+B3+2*B2)
490 P[I]=(R1^2+I1^2)/(R3^2+I3^2)
500 PLOT Y,P[I]
510 NEXT I
520 PEN
530 GOTO 220
540 END

```

Program in File 7

This program allows the influence of the embedding network on the mixer conversion loss to be predicted. It is known from ideal mixer theory that the Y-, Z-, G-, or H-type mixer with a short-circuited, open-circuited, or resistively-terminated image-frequency signal presents a certain resistance R_{RF} at signal frequency, which value is dependent on the characteristic of the nonlinear element, pump power level, and type of mixer. For a given type of mixer, the value of R_{RF} can be predicted from measurement of the resistance R_{IF} presented by the mixer at I.F.

The program in File 7 computes the minimum transducer loss (with respect to the backshort position) for a given embedding network, frequency, and ideal mixer R.F. resistance R_{RF} . It assumes that the signal source is perfectly matched to the waveguide. The loss component due to the reflection, the optimum position of the backshort, and the impedance $Z_p = R_p + jX_p$ presented by the outside circuit to the ideal mixer at this backshort position, are also printed.

The program listing and an example of printout during execution follows.

```

WAVEGUIDE DIMENSIONS IN MILS      A= 51.0      B= 6.4
FREQUENCY: START= 150.00GHZ      STOP= 160.00      DELTA= 1.00GHZ
IDEAL MIXER RF RESISTANCE= 200.0 OHM
INDUCTANCE= 0.110NH      CAPACITANCE= 5.10FF
DIODE RESISTANCE= 24.90 OHM      POST CAPACITANCE= 6.60 FF
TRANSFORMER TURNS RATIO= 0.90
  F(GHZ)      P TRAN(DB)      P REF(DB)      RP(OHM)      XP(OHM)      BS(MIL)
 150.00      0.65      0.13      252.55      -335.61      14.5
 151.00      0.65      0.13      250.54      -334.30      14.4
 152.00      0.65      0.13      248.60      -332.95      14.3
 153.00      0.65      0.12      246.71      -331.58      14.1
 154.00      0.65      0.12      244.87      -330.18      14.0
 155.00      0.65      0.12      243.07      -328.77      13.9
 156.00      0.65      0.12      241.32      -327.34      13.8
 157.00      0.66      0.11      239.60      -325.90      13.7
 158.00      0.66      0.11      237.92      -324.46      13.5
 159.00      0.66      0.11      236.27      -323.02      13.4
 160.00      0.66      0.11      234.64      -321.58      13.3

```

```

10 DISP "WAVEGUIDE DIMENSIONS IN MILS A,B";
20 INPUT A,B
30 WRITE (15,110)A,B
40 DISP "FREQUENCY:START,STOP,DELTA";
50 INPUT F1,F2,F3
60 WRITE (15,90)F1,F2,F3
70 FORMAT "INDUCTANCE=",F6.3,"NH",3X,"CAPACITANCE=",F6.2,"FF"
80 FORMAT "DIODE RESISTANCE=",F6.2," OHM",3X,"POST CAPACITANCE=",F6.
90 FORMAT "FREQUENCY: START=",F7.2,"GHZ",5X,"STOP=",F7.2,5X,"DELTA="
100 FORMAT "IDEAL MIXER RF RESISTANCE=",F7.1," OHM"
110 FORMAT "WAVEGUIDE DIMENSIONS IN MILS",5X,"A=",F5.1,4X,"B=",F5.1
120 DISP "IDEAL MIXER RF RESISTANCE";
130 INPUT R5
140 WRITE (15,100)R5
150 DISP "WSKR. IND., DIODE CAP.=";
160 INPUT L,C
170 WRITE (15,70)L,C
180 DISP "DIODE RESISTANCE,POST CAPACITANCE=";
190 INPUT R,C2
200 WRITE (15,80)R,C2
210 DISP "TRANSFORMER TURNS RATIO=";
220 INPUT K
230 WRITE (15,240)K
240 FORMAT "TRANSFORMER TURNS RATIO=",F5.2
250 PRINT " F(GHZ)      P TRAN(DB)      P REF(DB)      RP(OHM)      XP(OHM)
260 M1=INT((F2-F1)/F3)
270 F1=F1-F3
280 FOR M=1 TO M1+1
290 F1=F1+F3
300 B1=2*PI*F1*C*1E-06
310 X1=2*PI*F1*L
320 B2=X1/(R↑2+X1↑2)
330 G=R/(R↑2+X1↑2)
340 B3=B1-B2
350 G1=1/R5
360 G2=G↑2-B2↑2
370 G3=G1+G
380 G5=G3↑2+B3↑2
390 B4=(-B3*G2-2*G*B2*G3)/G5
400 A2=SQR(1-(1.1811E+04/(F1*A↑2))↑2)
410 A1=A*A2*K↑2/(376.73*B↑2)
420 G4=A1+G
430 G6=G4↑2+B4↑2
440 R1=G1*A1+G*G4+B2↑2-B4*B3
450 I1=B4*G1+B3*A1+G*(B4+B3+2*B2)
460 P1=-10*LGT(4*G1*A1*(G↑2+B2↑2)/(R1↑2+I1↑2))
470 R2=G-(G2*G3-2*B2*B3*G)/G5
480 S1=-10*LGT(1-((A1-R2)/(A1+R2))↑2)
490 R3=G-(G2*G4-2*G*B2*B4)/G6
500 I3=B3+(B4*G2+2*G*B2*G4)/G6
510 Y=B4+B2-2*PI*F1*C2*1E-06
520 L1=1.1811E+04/(A2*F1)
530 Y1=ATN(-A1/Y)
540 L2=Y1*L1/(2*PI)+(1-SGN(Y1))*L1/4
550 WRITE (15,560)F1,P1,S1,1/R3,-1/I3,L2
560 FORMAT F7.2,4X,F7.2,6X,F7.2,4X,F9.2,3X,F9.2,3X,F6.1
570 NEXT M
580 END

```

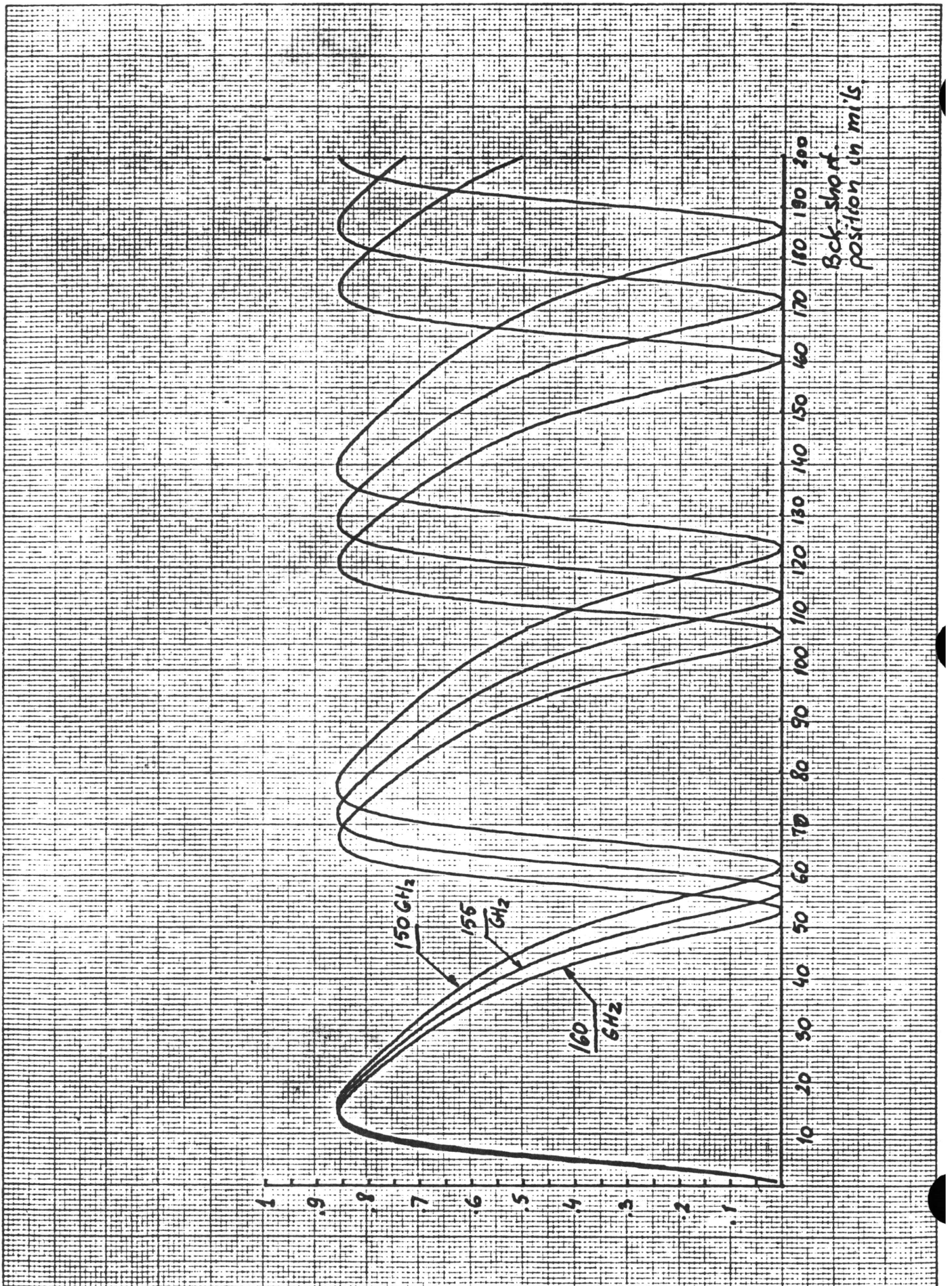
Program in File 8

This program computes and plots the transducer attenuation of the embedding network for a given frequency and ideal mixer R.F. resistance versus position of the backshort. It allows the positions of the backshort to be found at which good SSB or DSB performance may be expected. The program assumes that the signal source is perfectly matched to the waveguide.

The program listing and examples of the printout and plot follows.

```
WAVEGUIDE DIMENSIONS IN MILS      A= 51.0      B= 6.4
IDEAL MIXER RF RESISTANCE= 200.0 OHM
INDUCTANCE= 0.110NH      CAPACITANCE= 5.10FF
DIODE RESISTANCE= 24.90      POST CAPACITANCE= 6.60 FF
TRANSFORMER TURNS RATIO= 0.90
BACK SHORT(MILS):START= 0.0      STOP= 200.0      DELTA= 1.0
FREQUENCY= 150.00GHZ
MINIMUM TRANSDUCER ATTENUATION= 0.647 DB

FREQUENCY= 155.00GHZ
MINIMUM TRANSDUCER ATTENUATION= 0.653 DB
FREQUENCY= 160.00GHZ
MINIMUM TRANSDUCER ATTENUATION= 0.665 DB
```



```

10 DISP "WAVEGUIDE DIMENSIONS IN MILS A,B";
20 INPUT A,B
30 WRITE (15,80)A,B
40 FORMAT "INDUCTANCE=",F6.3,"NH",3X,"CAPACITANCE=",F6.2,"FF"
50 FORMAT "DIODE RESISTANCE=",F6.2,3X,"POST CAPACITANCE=",F6.2," FF"
60 FORMAT "FREQUENCY=",F7.2,"GHZ"
70 FORMAT "IDEAL MIXER RF RESISTANCE=",F7.1," OHM"
80 FORMAT "WAVEGUIDE DIMENSIONS IN MILS",5X,"A=",F5.1,4X,"B=",F5.1
90 DISP "IDEAL MIXER RF RESISTANCE";
100 INPUT R5
110 WRITE (15,70)R5
120 DISP "MSKR. IND., DIODE CAP.=";
130 INPUT L,C
140 WRITE (15,40)L,C
150 DISP "DIODE RESISTANCE,POST CAPACITANCE=";
160 INPUT R,C2
170 WRITE (15,50)R,C2
180 DISP "TRANSFORMER TURNS RATIO=";
190 INPUT K
200 WRITE (15,210)K
210 FORMAT "TRANSFORMER TURNS RATIO=",F5.2
220 DISP "BACK SHORT: START,STOP,DELTA";
230 INPUT L1,L2,L3
240 WRITE (15,250)L1,L2,L3
250 FORMAT "BACK SHORT(MILS):START=",F6.1,3X,"STOP=",F6.1,3X,"DELTA=",F6.1
260 SCALE L1,L2,0,1
270 AXIS L1,10
280 YAXIS 0,0,05
290 MI=INT((L2-L1)/L3)
300 DISP "FREQUENCY";
310 INPUT F1
320 WRITE (15,60)F1
330 B1=2*PI*F1*C*1E-06
340 X1=2*PI*F1*L
350 B2=X1/(R1+X1*12)
360 GR/(R1+X1*12)
370 B5=2*PI*F1*C2*1E-06
380 B3=B1-B2
390 B6=B5-B2
400 G1=1/R5
410 G2=G12-B2*2
420 G3=G1+G
430 G5=G3+2+B3*2
440 B4=(-B3*G2-2*G*B2*G3)/G5
450 R2=SQRT(1-(1.1811E+04/(F1*A*2)))*2)
460 A1=A*A2*K*2/(376.73*B*2)
470 G4=A1+G
480 R1=G1*A1+G*G4+B2*2-B4*B3
490 I1=B4*G1+B3*A1+G*(B4+B3+2*B2)
500 D1=4*G1*A1*(G1+2*B2*2)
510 P1=-10*LGT(D1/(R1*2+I1*2))
520 WRITE (15,530)P1
530 FORMAT "MINIMUM TRANSDUCER ATTENUATION=",F8.3," DB"
540 FOR M=1 TO M1
550 L4=L1+L3*M
560 Y=L4*A2*F1*PI/5.9055E+03
570 B4=B6-A1*COS(Y)/SIN(Y)
580 R1=G1*A1+G*G4+B2*2-B4*B3
590 I1=B4*G1+B3*A1+G*(B4+B3+2*B2)
600 D2=R1*2+I1*2
610 P2=D1/D2
620 PLOT L4,P2
630 NEXT M
640 PEN
650 GOTO 300
660 END

```


Program in File 9

In some cases it is interesting to know if there exists a position of the backshort for which the embedding circuit presents a real impedance to the ideal mixer; the value of this resistance is also of interest.

This question is examined by the program listed, with an example of the printout during execution, on the next pages. The available attenuation of the embedding network is also computed for the position of the backshort that is found.

```
WAVEGUIDE DIMENSIONS IN MILLS      A= 51.0      B= 6.4
FREQUENCY: START= 150.00GHZ      STOP= 190.00      DELTA= 5.00GHZ
INDUCTANCE= 0.110NH      CAPACITANCE= 5.10FF
RESISTANCE= 24.900OHM
POST CAPACITANCE= 6.60 FF
TRANSFORMER TURNS RATIO= 0.90
F(GHZ)      R1(OHM)      P1(DB)      R2(OHM)      P2(DB)
150.00      X-RF NEVER IS EQUAL TO ZERO
155.00      X-RF NEVER IS EQUAL TO ZERO
160.00      X-RF NEVER IS EQUAL TO ZERO
165.00      X-RF NEVER IS EQUAL TO ZERO
170.00      X-RF NEVER IS EQUAL TO ZERO
175.00      231.52      6.54      155.65      4.18
180.00      295.34      7.73      147.46      3.48
185.00      363.95      8.87      145.12      3.02
190.00      442.82      10.19     145.07      2.66
```

```

M F[30],B[30,2],C[30,2],H[30,2],P[30,2]
SP "WAVEGUIDE DIMENSIONS IN MILLS A,B";
INPUT A,B
WRITE (15,120)A,B
SP "FREQUENCY:START,STOP,DELTA";
INPUT F1,F2,F3
WRITE (15,100)F1,F2,F3
FORMAT "INDUCTANCE=",F6.3,"NH",3X,"CAPACITANCE=",F6.2,"FF"
FORMAT "RESISTANCE=",F6.2,"OHM"
FORMAT "FREQUENCY: START=",F7.2,"GHZ",5X,"STOP=",F7.2,5X,"DELTA=",F6.2,5X
FORMAT "POST CAPACITANCE=",F6.2," FF"
FORMAT "WAVEGUIDE DIMENSIONS IN MILLS",5X,"A=",F5.1,4X,"B=",F5.1
FORMAT "TRANSFORMER TURNS RATIO=",F5.2
DISP "MSKR. IND., DIODE CAP.=";
INPUT L,C
WRITE (15,80)L,C
DISP "DIODE RESISTANCE=";
INPUT R
WRITE (15,90)R
DISP "POST CAPACITANCE=";
INPUT C2
WRITE (15,110)C2
DISP "TRANSFORMER TURNS RATIO=";
INPUT K
WRITE (15,130)K
PRINT "F(GHZ)      R1(OHM)      P1(DB)      R2(OHM)      P2(DB)
M1=INT((F2-F1)/F3)
FOR M=1 TO M1+1
F[M]=F1+(M-1)*F3
B1=2*PI*F[M]*C*1E-06
X1=2*PI*F[M]*L
B2=X1/(R↑2+X1↑2)
G=R/(R↑2+X1↑2)
B3=B1-B2
Z1=376.73*B*2/(A*SQR(1-(1.1811E+04/(F[M]*A*2))↑2)*K↑2)
B5=2*PI*F[M]*C2*1E-06
D1=(B2↑2-G↑2)↑2-4*B3*(B3*(G+1/Z1)↑2-2*B2*G*(G+1/Z1))
IF D1<0 THEN 490
FOR N=1 TO 2
B[M,N]=(G↑2-B2↑2+(-1)↑N*SQR(D1))/(2*B3)
C[M,N]=B[M,N]-B5+B2
H[M,N]=G-((G↑2-B2↑2)*(G+1/Z1)-2*B2*B[M,N]*G)/((G+1/Z1)↑2+B[M,N]↑2)
R1=H[M,N]/Z1+G*(1/Z1+H[M,N])+B2↑2-B[M,N]*B3
I1=B[M,N]*H[M,N]+B3/Z1+G*(B[M,N]+B3+2*B2)
P[M,N]=-10*LGT(4*H[M,N]*(G↑2+B2↑2)/(Z1*(R1↑2+I1↑2)))
NEXT N
WRITE (15,520)F[M],1/H[M,1],P[M,1],1/H[M,2],P[M,2]
GOTO 500
WRITE (15,510)F[M]
NEXT M
FORMAT F7.2,"      X-RF NEVER IS EQUAL TO ZERO"
FORMAT F7.2,5X,F9.2,6X,F7.2,5X,F9.2,6X,F7.2
END

```

Program in File 10

During experiments aimed at determining $\Delta B^{(k)}$ and $B_o^{(k)}$ for a given mixer mount and diode bias, the increase in the diode current ΔI and position of the backshort are usually recorded. This short program allows this data be plotted in $(\frac{\Delta I}{\Delta I_{\max}}, Y_{BS} \times Z_G)$ coordinates. This is of some help in determining the presence of large measurement errors, which make the curve asymmetrical. It can also increase the accuracy of the $\Delta B^{(k)}$ and $B_o^{(k)}$ measurements by graphical averaging. The program listing is shown below.

```
10 SCALE -10,10,0,1
20 XAXIS 0,1
30 YAXIS 0,0.05
40 DISP "HALF-WAVELENGTH IN MILLS=";
50 INPUT L
60 DISP "DELTA I MAX=";
70 INPUT D
80 DISP "DRIFT=";
90 INPUT X
100 FOR I=1 TO 200
110 DISP "BACKSHORT POSITION=";
120 INPUT S
130 DISP "DELTA I=";
140 INPUT A
150 PLOT -1/TAN(PI*S/L), (A-S*X/L)/D
160 IF S>L THEN 190
170 PEN
180 NEXT I
190 END
```

LISTING OF BACKSHORT ANALYSIS TAPE

0	3	2000	1791	10	900	0
1	3	2000	1955	10	1060	0
2	3	2000	1843	10	950	0
3	3	2000	1408	10	860	0
4	3	2000	1530	10	890	0
5	3	1500	1214	10	950	0
6	3	1000	736	10	540	0
7	3	1000	866	10	580	0
8	3	1000	812	10	660	0
9	3	1000	911	10	530	0
10	3	250	141	10	190	0
11	3	2500	1951	10	1030	0
12	0	2500	0	0	0	0